replication of SHIVrt/3rn reached a peak at about 19 days post-infection (p.i.) (Fig. 2a). This profile of kinetics was similar to that of NM-3rN, except that there was a slight delay in the initial rise in RT activity, indicating that SHIVrt/3rn could replicate well in this human $CD4^+$ cell line with almost the same replication competence as NM-3rN. In HSC-F cells, the replication of SHIVrt/3rn was delayed compared with that of NM-3rN and reached a peak at about 15 days p.i. (Fig. 2b). In monkey PBMCs, replication of SHIVrt/3rn reached a peak at about 22 days p.i. (Fig. 2c). Judging from the RT values, SHIVrt/3rn replicated to somewhat lower titres than NM-3rN. Nevertheless, it was clearly able to replicate in monkey PBMCs.

Effect of MKC-442, an HIV-1-specific non-nucleoside RT inhibitor, on virus growth

MKC-442 did not inhibit the replication of NM-3rN (which has the RT of SIV_{mac}) at any concentration examined, but it completely inhibited the replication of SHIVrt/3rn (which has the RT of HIV-1) at 200 nM (Fig. 3). In the presence of 20 nM MKC-442, growth of SHIVrt/3rn was initially blocked but, eventually, slow growth was observed approximately 10 days later compared with that at the start (in the absence of MKC-442) (Fig. 3b).

Replication of SHIVrt/3rn *in vivo*

To investigate the competence of SHIVrt/3rn to infect and replicate *in vivo*, we inoculated intravenously two female rhesus monkeys (MM251 and MM257) with the virus stock containing 1×10^5 $TCID_{50}$ per each monkey and performed virus isolation, DNA PCR, quantitative RT-PCR and FACScan analysis. Here we show the results obtained up to 32 weeks p.i.

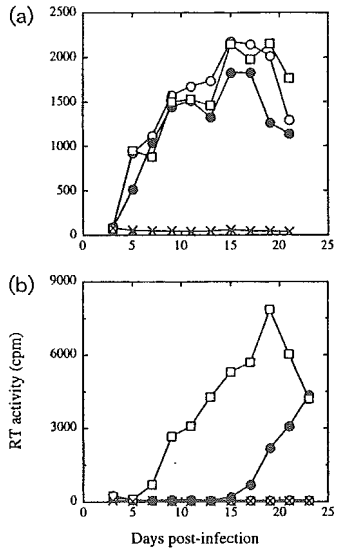

Fig. 3. Inhibition of the growth of NM-3rN (a) and SHIVrt/3rn (b) by MKC-442 in M8166 cells. Cell-free virus stocks from M8166 cells transfected with the respective chimeric DNA clones were infected in the presence of 20 nM (●) or 200 nM (○) MKC-442 and virion-associated RT activity in the culture supernatants was monitored every 2 days. □, Medium; ×, mock infection.

Firstly, we examined whether or not there were infected PBMCs that could generate infectious virus by co-culturing with M8166 cells (Table 1). From the PBMCs of MM251, infectious virus was isolated at 2 and 3 weeks p.i., and at 4 weeks p.i. from the PBMCs of MM257. To detect proviral DNA in the isolated PBMCs, we performed DNA PCR using the extracted chromosomal DNA from the PBMCs (Table 1). In the PBMCs from both MM251 and MM257, proviral DNA was detected constantly throughout the observation period, starting from 3 weeks p.i. until 32 weeks p.i. To determine plasma viral RNA loads, we extracted RNA from the isolated plasma samples and performed quantitative RT-PCR (Fig. 4a). The plasma viral RNA loads of MM251 exhibited a peak during 2 to 3 weeks p.i., and those of MM257 did so during 3–4 weeks p.i. The number of RNA copies at the peak period was $2{\cdot}6 \times 10^4$ and $1{\cdot}2 \times 10^4$ copies ml^{-1}, respectively. As for MM251, viral RNA was detected in the plasma samples up to 10 weeks p.i. On the other hand, no viral RNA was detected in the plasma samples of MM257 after 6 weeks p.i. To detect and titrate antibodies against HIV-1, we measured particle agglutination antibody titres using the Serodia HIV-1/2 kit (Fujirebio) (Table 1). Antibodies were detected in both

Table 1. Virological and immunological status of SHIVrt/3rn-inoculated monkeys

	DNA PCR*		Virus isolation†		Antibody titre‡	
Week	MM251	MM257	MM251	MM257	MM251	MM257
0	−	−	ND	ND	ND	ND
1	−	−	−	−	ND	ND
2	−	−	+	−	<32	<32
3	+	+	+	−	128	128
4	+	+	−	+	512	128
6	+	+	−	−	2048	256
8	+	+	−	−	2048	512
10	+	+	−	−	2048	512
12	+	+	−	−	2048	512
16	+	+	−	−	2048	4096
20	+	+	−	−	4096	4096
26	+	+	−	−	4096	4096
32	+	+	−	−	4096	4096

*The presence of viral DNA in PBMCs was determined by PCR using primer pairs for amplification of the V3 region of HIV-1 *env*. +, Viral DNA detected; −, no viral DNA detected.

†Virus isolation was performed by co-culture of collected PBMCs and M8166 cells. +, Virus isolated; −, no virus isolated.

‡Antibody titres were measured by particle agglutination (Serodia HIV-1/2, Fujirebio).

ND, Not done.

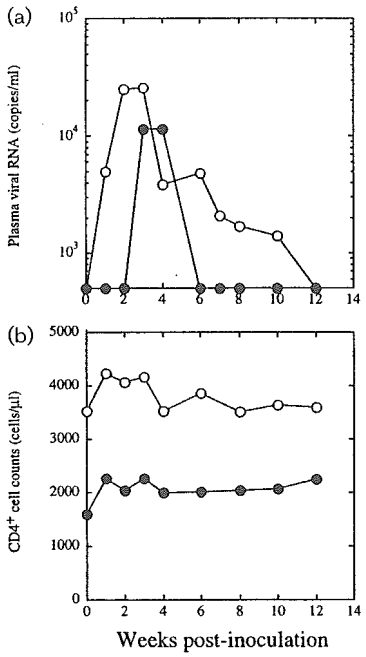

Fig. 4. (a) Plasma viral RNA loads of the SHIVrt/3rn-infected monkeys. Plasma viral RNA loads were measured by quantitative RT-PCR, as described in Methods. (b) Changes in the number of circulating $CD4^+$ cells with time. ○, MM251; ●, MM257.

monkeys first at 3 weeks p.i. and were maintained with high titres (4096) up to 32 weeks p.i. In addition, we analysed the number of $CD4^+$ cells in these rhesus monkeys after the inoculation. Both monkeys showed no significant decrease in the number of $CD4^+$ cells up to 32 weeks p.i. (Fig. 4b), suggesting that SHIVrt/3rn is non-pathogenic at this stage.

All of the above results indicate that SHIVrt/3rn could efficiently infect and replicate in rhesus monkeys and induce a humoral response against HIV-1 without causing any apparent symptoms of disease.

DISCUSSION

Most of the SHIVs constructed so far possess the 3′ half of the HIV-1 genome, including the *env* gene; the rest of the genome is from SIV. In this study, we constructed a new SHIV chimera, named SHIVrt/3rn, which has a broader HIV-1-derived region than any of the SHIVs reported previously. Specifically, SHIVrt/3rn differs from the previous SHIVs in that it carries part of the *pol* gene of HIV-1. SHIVrt/3rn replicated well, not only in established $CD4^+$ T-cell lines, such as M8166 and HSC-F, but also in monkey PBMCs (Fig. 2). Moreover, when it was inoculated into rhesus monkeys, it exhibited evidence of virus replication *in vivo* (Fig. 4 and Table 1). This virus has the *rt* region in addition to the 3′ part of the HIV-1genome, that is to say, *vpr*, *vpu*, *tat*, *rev*, *env* and *nef*. Therefore, it is genetically more close to HIV-1 than any of the other monkey-infecting SHIVs reported previously.

Since the newly constructed SHIVrt/3rn has the RT of HIV-1, we confirmed the inhibition of the replication of SHIVrt/3rn by an HIV-1-specific non-nucleoside-type RT inhibitor, MKC-442, *in vitro*. The 90 % effective concentration (EC_{90}) and the 50 % effective concentration (EC_{50}) of MKC-442 against HIV-1 were reported to be 98 and 15 nM, respectively (Baba *et al.*, 1994). EC_{90} and EC_{50} values were defined as the concentrations at which 90 and 50 % of HIV-1 induced CPE in MT-4 cells were protected (Pauwels *et al.*, 1988). In this study, the replication of SHIVrt/3rn was inhibited completely by MKC-442 at 200 nM. In addition, the initial rise in RT activity of SHIVrt/3rn was delayed by 20 nM MKC-442, which is considered to be a consequence of incomplete inhibition. (Fig. 3b). These results indicate that the sensitivity to MKC-442 of SHIVrt/3rn is similar to that of HIV-1, although it should be noted that different cells were employed for this inhibition assay. Today, highly active antiretroviral therapy, in which combinations of RT inhibitors and protease inhibitors are used, has shown satisfactory clinical benefits. Moreover, new anti-HIV drugs targeting other virus components, such as Env, are being developed. Since monotherapy resulted, in most cases, in failure, such entry blockers should be prescribed in combination with other drugs such as RT inhibitors. Having the RT and Env of HIV-1 and having a sensitivity to an RT inhibitor similar to that of HIV-1, SHIVrt/3rn can be used for the *in vivo* evaluation of a new combination therapy of HIV-1-specific RT inhibitors and entry blockers, such as CXCR4 antagonists, in monkeys.

Two rhesus monkeys were inoculated with 1×10^5 $TCID_{50}$ SHIVrt/3rn and both monkeys were infected consequently. The *in vivo* replication of NM-3rn, the parental molecular clone of SHIVrt/3rn, was reported previously (Bogers *et al.*, 1997). According to that report, eight rhesus monkeys were inoculated with NM-3rn at six different virus titres, ranging from $6{\cdot}3 \times 10^3$ to $6{\cdot}3 \times 10^{-1}$ $TCID_{50}$. Seven of the eight monkeys were infected with NM-3rn. Viruses were isolated continuously from 2 to 12 weeks p.i. from five of the seven infected monkeys. In this study, we also performed virus isolation. However, we could isolate viruses only at 2 and 3 weeks p.i. from one of the two monkeys and at 4 weeks p.i. from the other (Table 1). In the case of NM-3rn infection, the results of DNA PCR showed the presence of proviral DNA from all seven monkeys infected with NM-3rn at 2 and 4 weeks p.i. and from all three monkeys analysed out of the seven at 8 weeks p.i. In this study, we also performed DNA PCR and could detect proviral DNA constantly, starting at 3 weeks p.i., from both of the monkeys, although we could not detect it at 2 weeks p.i. (Table 1). These results suggest that SHIVrt/3rn possesses a slightly lower replication competence *in vivo* than NM-3rn. This weak replication competence was also observed *in vitro*, as shown by the growth kinetics in monkey PBMCs (Fig. 2c). The replacement of the *rt* region of SIV with that of HIV-1 might have affected the replication potential of the virus.

Überla *et al.* (1995) constructed a SHIV having the *rt* region

of HIV-1 and the rest of the genome from SIV_{mac} (RT-SHIV). Two rhesus monkeys inoculated with RT-SHIV exhibited a systemic infection and one of them developed an AIDS-like symptom at approximately 6 months p.i. This result suggested that RT-SHIV possessed a higher replication competence *in vivo* than SHIVrt/3rn. This difference may be because SHIVrt/3rn and RT-SHIV use different strains of HIV-1 for the *rt* region, or because SHIVrt/3rn has a broader HIV-1-derived region, one that covers the region from *vpr* to *nef*. Although the reason for the lower replication competence of SHIVrt/3rn is not clear at this stage, we expect that it can be improved by serial animal passages and/or by using different strains of HIV-1.

We are now attempting to make new SHIVs in which the HIV-1-derived region is as broad as possible, without losing the infectivity of the virus to monkeys. We hope this will allow us to establish a novel animal model that ultimately mimics HIV-1 infection in humans and to identify the virus determinants of the species tropism of HIV-1, namely, the virus factors that restrict HIV-1 replication in monkey cells.

ACKNOWLEDGEMENTS

We thank Dr Masanori Baba for providing MKC-442. This work was supported by a grant-in-aid for AIDS research from the Japanese Ministry of Education, Culture, Sports, Science and Technology and the Japanese Ministry of Health, Labour and Welfare and Research Grant on Health Sciences focusing on Drug Innovation from Japan Health Sciences Foundation.

REFERENCES

Adachi, A., Gendelman, H. E., Koenig, S., Folks, T., Willey, R., Rabson, A. & Martin, M. A. (1986). Production of acquired immunodeficiency syndrome-associated retrovirus in human and nonhuman cells transfected with an infectious molecular clone. *J Virol* **59**, 284–291.

Akari, H., Mori, K., Terao, K., Otani, I., Fukasawa, M., Mukai, R. & Yoshikawa, Y. (1996). *In vitro* immortalization of Old World monkey T lymphocytes with herpesvirus saimiri: susceptibility to infection with simian immunodeficiency viruses. *Virology* **218**, 382–388.

Baba, M., Shigeta, S., Yuasa, S. & 7 other authors (1994). Preclinical evaluation of MKC-442, a highly potent and specific inhibitor of human immunodeficiency virus type 1 *in vitro*. *Antimicrob Agents Chemother* **38**, 688–692.

Bogers, W. M., Dubbes, R., ten Haaft, P. & 12 other authors (1997). Comparison of *in vitro* and *in vivo* infectivity of different clade B HIV-1 envelope chimeric simian/human immunodeficiency viruses in *Macaca mulatta*. *Virology* **236**, 110–117.

Clapham, P. R., Weiss, R. A., Dalgleish, A. G., Exley, M., Whitby, D. & Hogg, N. (1987). Human immunodeficiency virus infection of monocytic and T-lymphocytic cells: receptor modulation and differentiation induced by phorbol ester. *Virology* **158**, 44–51.

Daniel, M. D., Kirchhoff, F., Czajak, S. C., Sehgal, P. K. & Desrosiers, R. C. (1992). Protective effects of a live attenuated SIV vaccine with a deletion in the *nef* gene. *Science* **258**, 1938–1941.

Fultz, P. N., McClure, H. M., Daugharty, H., Brodie, A., McGrath, C. R., Swenson, B. & Francis, D. P. (1986). Vaginal transmission of human immunodeficiency virus (HIV) to a chimpanzee. *J Infect Dis* **154**, 896–900.

Gajdusek, D. C., Amyx, H. L., Gibbs, C. J., Jr & 7 other authors (1985). Infection of chimpanzees by human T-lymphotropic retroviruses in brain and other tissues from AIDS patients. *Lancet* **i**, 55–56.

Harouse, J. M., Gettie, A., Tan, R. C., Blanchard, J. & Cheng-Mayer, C. (1999). Distinct pathogenic sequela in rhesus macaques infected with CCR5 or CXCR4 utilizing SHIVs. *Science* **284**, 816–819.

Hayami, M., Igarashi, T., Kuwata, T., Ui, M., Haga, T., Ami, Y., Shinohara, K. & Honda, M. (1999). Gene-mutated HIV-1/SIV chimeric viruses as AIDS live attenuated vaccines for potential human use. *Leukemia* **13** (Suppl. 1), S42–S47.

Igarashi, T., Shibata, R., Hasebe, F. & 7 other authors (1994). Persistent infection with SIV_{mac} chimeric virus having *tat*, *rev*, *vpu*, *env* and *nef* of HIV type 1 in macaque monkeys. *AIDS Res Hum Retroviruses* **10**, 1021–1029.

Igarashi, T., Kuwata, T., Takehisa, J. & 7 other authors (1996). Genomic and biological alteration of a human immunodeficiency virus type 1 (HIV-1)-simian immunodeficiency virus strain mac chimera, with HIV-1 Env, recovered from a long-term carrier monkey. *J Gen Virol* **77**, 1649–1658.

Joag, S. V., Li, Z., Foresman, L., Stephens, E. B., Zhao, L. J., Adany, I., Pinson, D. M., McClure, H. M. & Narayan, O. (1996). Chimeric simian/human immunodeficiency virus that causes progressive loss of $CD4^+$ T cells and AIDS in pig-tailed macaques. *J Virol* **70**, 3189–3197.

Joag, S. V., Li, Z., Foresman, L. & 10 other authors (1997). Characterization of the pathogenic KU-SHIV model of acquired immunodeficiency syndrome in macaques. *AIDS Res Hum Retroviruses* **13**, 635–645.

Kestler, H. W. D., III, Ringler, D. J., Mori, K., Panicali, D. L., Sehgal, P. K., Daniel, M. D. & Desrosiers, R. C. (1991). Importance of the *nef* gene for maintenance of high virus loads and for development of AIDS. *Cell* **65**, 651–662.

Kozyrev, I. L., Miura, T., Takemura, T., Kuwata, T., Ui, M., Ibuki, K., Iida, T. & Hayami, M. (2002). Co-expression of interleukin-5 influences replication of simian/human immunodeficiency viruses *in vivo*. *J Gen Virol* **83**, 1183–1188.

Kuwata, T., Igarashi, T., Ido, E., Jin, M., Mizuno, A., Chen, J. & Hayami, M. (1995). Construction of human immunodeficiency virus 1/simian immunodeficiency virus strain mac chimeric viruses having *vpr* and/or *nef* of different parental origins and their *in vitro* and *in vivo* replication. *J Gen Virol* **76**, 2181–2191.

Letvin, N. L., Daniel, M. D., Sehgal, P. K. & 7 other authors (1985). Induction of AIDS-like disease in macaque monkeys with T-cell tropic retrovirus STLV-III. *Science* **230**, 71–73.

Li, J., Lord, C. I., Haseltine, W., Letvin, N. L. & Sodroski, J. (1992). Infection of cynomolgus monkeys with a chimeric HIV-1/SIV_{mac} virus that expresses the HIV-1 envelope glycoproteins. *J Acquir Immune Defic Syndr* **5**, 639–646.

Naidu, Y. M., Kestler, H. W. D., III, Li, Y. & 8 other authors (1988). Characterization of infectious molecular clones of simian immunodeficiency virus (SIV_{mac}) and human immunodeficiency virus type 2: persistent infection of rhesus monkeys with molecularly cloned SIV_{mac}. *J Virol* **62**, 4691–4696.

Novembre, F. J., Saucier, M., Anderson, D. C. & 7 other authors (1997). Development of AIDS in a chimpanzee infected with human immunodeficiency virus type 1. *J Virol* **71**, 4086–4091.

Pauwels, R., Balzarini, J., Baba, M., Snoeck, R., Schols, D., Herdewijn, P., Desmyter, J. & De Clercq, E. (1988). Rapid and

automated tetrazolium-based colorimetric assay for the detection of anti-HIV compounds. *J Virol Methods* **20**, 309–321.

Reimann, K. A., Li, J. T., Veazey, R., Halloran, M., Park, I. W., Karlsson, G. B., Sodroski, J. & Letvin, N. L. (1996). A chimeric simian/human immunodeficiency virus expressing a primary patient human immunodeficiency virus type 1 isolate *env* causes an AIDS-like disease after *in vivo* passage in rhesus monkeys. *J Virol* **70**, 6922–6928.

Shibata, R., Kawamura, M., Sakai, H., Hayami, M., Ishimoto, A. & Adachi, A. (1991). Generation of a chimeric human and simian immunodeficiency virus infectious to monkey peripheral blood mononuclear cells. *J Virol* **65**, 3514–3520.

Überla, K., Stahl-Hennig, C., Bottiger, D. & 7 other authors (1995). Animal model for the therapy of acquired immunodeficiency syndrome with reverse transcriptase inhibitors. *Proc Natl Acad Sci U S A* **92**, 8210–8214.

Ui, M., Kuwata, T., Igarashi, T. & 9 other authors (1999). Protection of macaques against a SHIV with a homologous HIV-1 Env and a pathogenic SHIV-89.6P with a heterologous Env by vaccination with multiple gene-deleted SHIVs. *Virology* **265**, 252–263.

Veazey, R. S., DeMaria, M., Chalifoux, L. V. & 7 other authors (1998). Gastrointestinal tract as a major site of $CD4^+$ T cell depletion and viral replication in SIV infection. *Science* **280**, 427–431.

Willey, R. L., Smith, D. H., Lasky, L. A., Theodore, T. S., Earl, P. L., Moss, B., Capon, D. J. & Martin, M. A. (1988). *In vitro* mutagenesis identifies a region within the envelope gene of the human immunodeficiency virus that is critical for infectivity. *J Virol* **62**, 139–147.

Yuasa, S., Sadakata, Y., Takashima, H., Sekiya, K., Inouye, N., Ubasawa, M. & Baba, M. (1993). Selective and synergistic inhibition of human immunodeficiency virus type 1 reverse transcriptase by a non-nucleoside inhibitor, MKC-442. *Mol Pharmacol* **44**, 895–900.

Available online at www.sciencedirect.com
SCIENCE DIRECT®
Journal of Virological Methods 112 (2003) 121–128
Journal of Virological Methods
www.elsevier.com/locate/jviromet

The impact of highly active antiretroviral therapy by the oral route on the CD8 subset in monkeys infected chronically with $SHIV_{89.6P}$

Kazuhisa Yoshimura [a], Eiji Ido [c], Hisashi Akiyama [c], Tetsuya Kimura [a], Manabu Aoki [b], Hajime Suzuki [c], Hiroaki Mitsuya [b], Masanori Hayami [c], Shuzo Matsushita [a,*]

[a] *Division of Clinical Retrovirology and Infectious Diseases, Center for AIDS Research, Kumamoto University, 2-2-1 Honjo, Kumamoto 860-0811, Japan*
[b] *Department of Internal Medicine II, Kumamoto University, Kumamoto 860-0811, Japan*
[c] *The Laboratory of Viral Pathogenesis, Institute for Virus Research, Kyoto University, Kyoto 606-8507, Japan*

Received 27 March 2003; received in revised form 25 June 2003; accepted 26 June 2003

Abstract

The objective of this study was to assess the impact of highly active antiretroviral therapy (HAART) by an oral route on the peripheral blood CD8 subset in the monkeys infected persistently with a pathogenic strain, $SHIV_{89.6P}$. Two rhesus macaques were inoculated intravenously with $SHIV_{89.6P}$, then treated with the combination of AZT, 3TC and Lopinavir/Ritonavir (LPV/RTV) as recommended in humans by the oral route with confectionery continued for 28 days. In one of two chronically infected macaques, MM260, the viral load was maintained in the range of 10^4–10^5 copies/ml before HAART. The plasma viral load and proviral DNA decreased dramatically during the treatment, and cessation of this therapy the viral load rebounded to the pre-treatment level but the proviral DNA rebound was delayed. The other monkey, MM242, had low viral loads ($1.2 \times 10^3 - < 5 \times 10^2$ copies/ml) both before and after HAART. $CD4^+$ and $CD8^+$ T cell counts and proviral DNA level were not significantly changed after the treatment. The percentages of $CD8^+CD45RA^-Ki67^+$ cells increased during (MM260) or after (MM242) HAART and the subset was maintained at a high percentage until 18 weeks post HAART in MM242. These findings suggest that this primate model might serve an important role in testing the virological and immunological efficacy of novel therapeutic strategies combined with HAART.

Keywords: $SHIV_{89.6P}$; Antiretroviral therapy; $Ki67^+$; Memory $CD8^+$ T cells; Proviral DNA; Animal model

1. Introduction

Pre-clinical approaches in non-human primate models of AIDS enable pertinent evaluations to be carried out and the possibility to determine precisely the conditions of efficacy can be determined (Le Grand et al., 1994). Macaques infected with pathogenic strains of the simian immunodeficiency virus (SIV) or related chimeras expressing the envelope of HIV-1 (simian/human immunodeficiency virus, SHIV) are currently relevant models of human HIV infection and AIDS (Haigwood, 1999; Nath et al., 2000; Nathanson et al., 1999; Tang et al., 2002). SIV and SHIV have biological properties similar to those of HIV, and infection of macaques with pathogenic isolates induces an immunodeficiency syndrome strikingly mimicking human AIDS (Reimann et al., 1996a,b). Animal models are also useful for understanding the complexity of the pathogenic mechanisms of HIV infection during antiviral treatment (Endo et al., 2000; Enose et al., 2002; Igarashi et al., 2001).

SHIVs contain HIV-1-derived segments encoding viral envelope glycoproteins and regulatory proteins such as Tat, Rev and Vpu in the SIV background (Li et al., 1992). SHIV containing the envelope glycoproteins of a primary HIV-1 isolate, 89.6, replicated in rhesus monkeys but did not deplete $CD4^+$ T lymphocytes or induce disease in these animals. Serial transfer

* Corresponding author. Tel.: +81-96-373-6536; fax: +81-96-373-6537.
E-mail address: shuzo@kaiju.medic.kumamoto-u.ac.jp (S. Matsushita).

0166-0934/03/$ - see front matter © 2003 Elsevier B.V. All rights reserved.
doi:10.1016/S0166-0934(03)00201-5

of blood from $SHIV_{89.6}$-infected monkeys to naive monkeys generated a virus, termed $SHIV_{89.6P}$, that exhibited only a modest increase in replication in infected monkeys compared with $SHIV_{89.6}$. However, $SHIV_{89.6P}$ caused rapid loss of $CD4^+$ T lymphocytes and, subsequently, AIDS-like illness in inoculated monkeys (Reimann et al., 1996a,b). An animal system using $SHIV_{89.6P}$ acutely infected macaques with highly active antiretroviral therapy (HAART) was the same regimen used for humans (AZT+3TC+IDV) by the oral route (Le Grand et al., 2002, 2000; Thiebot et al., 2001) and a nasogastric catheter was placed for administering the drugs (Thiebot et al., 2001).

The objective of this study was to set up a novel AIDS model in monkeys and to evaluate the efficacy of the combination of AZT, 3TC and Lopinavir/Ritonavir (LPV/RTV), when administered by the oral route to the monkeys infected chronically with the pathogenic $SHIV_{89.6P}$.

2. Materials and methods

2.1. Cells and viruses

M8166 cells (Clapham et al., 1987) were grown in an RPMI-1640-based culture medium supplemented with 15% fetal calf serum (FCS: HyClone Laboratories, Logan, UT), 50 U/ml of penicillin and 50 mg/ml of streptomycin. $SHIV_{89.6P}$ (Reimann et al., 1996a) and $HIV\text{-}1_{LAI}$ (Clavel et al., 1986) were used for the drug susceptibility assay.

2.2. Antiviral agents

Zidovudine (AZT) was purchased from Sigma (St. Louis, MO). Lamivudine (3TC) was a kind gift from R.F. Schinazi (Atlanta, GA). RTV was kindly provided by Abbott Laboratories (Abbott Park, Ill.). LPV was synthesized using published methods (Carrillo et al., 1998). Kaletra™ liquid (LPV/RTV) and Combivir® tablets (AZT/3TC) were purchased from Abbott Laboratories and GlaxoSmithKline, respectively.

2.3. Drug susceptibility assay

The sensitivities of $SHIV_{89.6P}$ against various drugs were determined as described previously with minor modifications (Maeda et al., 2001; Yoshimura et al., 1999). Briefly, M8166 cells (5×10^3 per ml) were exposed to 100 $TCID_{50}$ of $SHIV_{89.6P}$ and $HIV\text{-}1_{LAI}$, in the presence of various concentrations of drugs in 96-well microculture plates and incubated at 37 °C for 7 days. After 100 μl of the medium was removed from each well, 10 μl of 3-(4,5-dimetylthiazol-2-yl)-2,5-diphenyltetrazolium bromide (MTT) solution (7.5 mg/ml) in phosphate-buffered saline (PBS) was added to each well in the plate, followed by incubation at 37 °C for 2 h. After incubation, to dissolve the formazan crystals, 100 μl of acidified isopropanol containing 4% (v/v) Triton X-100 was added to each well and the optical density was measured in a microplate reader. All assays were performed in duplicate (S.D.: $<25\%$).

2.4. Monkeys

Two rhesus macaques (*Macaca mulatta*), MM260 and MM242, were infected intravenously with 1000 and 10 $TCID_{50}$ (50% tissue culture infectious dose) of a pathogenic $SHIV_{89.6P}$, respectively. $SHIV_{89.6P}$ was provided by K.A. Reimann and N.L. Letvin (Beth Israel Hospital, Boston, MA). However, because the stock $SHIV_{89.6P}$, which was not the original virus used in this study might have slight loss of pathogenicity in the course of stock virus preparation, the CD4 values of the monkeys inoculated with $SHIV_{89.6P}$ sometimes showed a some reversal (20–50% of the mean value before inoculation) after the drastic drop up to 10% at 2–3 weeks post inoculation. The two animals were treated with a combination of AZT (5 mg/kg), 3TC (2.5 mg/kg) and LPV/RTV (12/3 mg/kg) administered by the oral route with confectionery twice a day after an intravenous inoculation of $SHIV_{89.6P}$. Briefly, Combivir tablets (AZT/3TC) were ground and mixed with Kaletra™ liquid (LPV/RTV) then the drug-mixture was poured into the sweet confectionery that the monkeys are fond of. We monitored the compliance of drug delivery by observing the monkeys until they had finished eating the sweets. Treatment was initiated 38 (MM260) or 84 (MM242) weeks after the inoculation of $SHIV_{89.6P}$, and was continued for 28 days. Two uninfected, untreated animals (MM132 and MM244) were used as controls (Fig. 3A and C). Blood samples were collected periodically from the infected and healthy macaques for analysis of $CD4^+$ and $CD8^+$ cell counts, $Ki67^+$ percentage, viral loads, and proviral DNA.

2.5. Measuring of proviral DNA level

Proviral DNA levels in peripheral blood mononuclear cells (PBMC) from $SHIV_{89.6P}$-infected-monkey were measured using a novel hypersensitive nested PCR in the LTR region. The first PCR was carried out with SHIV-O-S (5′-AGGCATCATACCAGATTGGCA-3′) and SHIV-O-A (5′-ATTGAAGAGGGCTTTAAGCAA-3′) primers in the U3/R region. The first PCR reaction mixture consisted of 0.5 μg of the proviral DNA solution, 50 mM KCl, 10 mM Tris–HCl (pH 8.0), 2 mM $MgCl_2$, 0.01% gelatin, 0.2 mM dNTPs, 1.5 U of EX Taq DNA polymerase (Takara Shuzo Co., LTD.), and 15 pmol of each of the first PCR primers in a total volume of 30 μl. The PCR conditions used were an

initial 3 min at 94 °C, followed by 24 cycles of 30 s at 94 °C, 30 s at 65 °C, and 1 min at 70 °C with a final 10 min extension at 72 °C. The first PCR product was subsequently diluted 1000-fold, and subjected to a real-time PCR assay for measuring U3 DNA using SHIV-I-S (5′-AGACATTTGGCTGGCTATGGA-3′), SHIV-I-A (5′-AAGTTTGAGCTGGATGCATTA-3′) and SYBR Green PCR Master Mix (Perkin–Elmer-Applied Biosystems). For amplification and detection of PCR products we preheated the samples at 50 °C for 2 min and at 95 °C for 10 min, followed by 40 cycles of denaturation at 95 °C for 15 s and annealing/extension at 60 °C for 30 s, using an ABI PRISM 7700 sequence detection system (Perkin–Elmer-Applied Biosystems). The SIVmac239 LTR sequence was cloned into pCR2.1 TOPO vector (Invitrogen), and served as a standard curve. The level of SHIV DNA was expressed as copies per micrograms of cellular DNA (copies/μg DNA). Under these conditions, the detection limit was 300 copies/μg DNA.

2.6. Detection of plasma viral RNA

Plasma viral loads were determined using Taqman RT-PCR kits (Perkin–Elmer, New Jersey, USA) and ABI Prism 7700 (Ui et al., 1999). Absolute copy numbers of viral RNAs were determined using standard plasma samples, the copy numbers, of which were determined by Chiron Corporation. Under these conditions, the detection limit was 500 copies/ml.

2.7. FACS analysis

Whole blood samples of the monkeys were stained with fluorecently labeled mouse monoclonal antibodies as follows; phycoerythrin (PE)-conjugated anti-human CD4 (NU-$T_{H/N}$, Nichirei, Japan), PerCP-conjugated anti-human CD8 monoclonal antibody (Leu-2a, BD PharMingen, CA). After hemolysis of the blood using a lysing solution (BD PharMingen), the, respectively, labeled lymphocytes were analyzed using FACSCalibur (BD PharMingen).

PBMCs were also isolated from the macaques using centrifugation on Ficoll–Hypaque density gradient centrifugation. The PBMCs were incubated with fluorochrome-labeled specific monoclonal antibodies against surface antigens, allophycocyanin (APC)-conjugated anti-human CD8 (RPA-T8, BD PharMingen) and PE-conjugated anti-human CD45RA (5H9, BD PharMingen), and also incubated with 7-amino-actinomycin D (7-AAD) (BD PharMingen) to exclude dead cells. After fixation and permeabilization, the cells were incubated with Ki67-FITC (B56, BD PharMingen). The stained cells were analyzed by four-color flow cytometry using a FACSCalibur (Kimura et al., 2002).

2.8. Statistical analysis

The $CD4^+$ and $CD8^+$ T cell counts between pre-HAART and baseline or post-HAART were determined statistically using Student's *t*-test.

3. Results

3.1. In vitro drug sensitivity of $SHIV_{89.6P}$ and HIV-1_{LAI}

We first tested two nucleoside reverse transcriptase inhibitors (NRTIs), AZT and 3TC, and two protease inhibitors (PIs), RTV and LPV, against $SHIV_{89.6P}$ and HIV-1_{LAI} in M8166 cells (Table 1). Antiviral activity of the two NRTIs was comparable against these two viruses. On the other hand, as shown in Table 1, $SHIV_{89.6P}$ had a high level of resistance to RTV (15–18-fold increase in IC_{50}) and a moderate level of resistance to LPV (5–6-fold) compared with the case against HIV-1_{LAI}. This finding is similar to a pattern of sensitivity of HIV-2 strains to PIs as reported (Yoshimura et al., 1999).

3.2. $SHIV_{89.6P}$-infected macaques were treated with HAART by the oral route

The replication of $SHIV_{89.6P}$ was inhibited by AZT, 3TC or LPV within the IC_{50} range between 0.007 and 0.47 μM in vitro (Table 1). We selected these three drugs for treatment to monkeys infected with $SHIV_{89.6P}$ because this combination is currently recommended for treatment of patients with HIV-1 infection. Two rhesus macaques were inoculated intravenously with 1000 and 10 $TCID_{50}$ of a cell-free stock of $SHIV_{89.6P}$ for MM260 and MM242, respectively. The monkeys, MM260 and MM242, became infected and were treated with HAART initiated at 38 and 64 weeks and continued until at 42 and 68 weeks post-inoculation, respectively. The animals were treated, as recommended in the case of humans, by the combination of AZT (5 mg/kg bid), 3TC (2.5 mg/kg bid) and LPV/RTV (12/3 mg/kg bid) after the intravenous inoculation of $SHIV_{89.6P}$. This treatment was administered by the oral route together with confectionery and was continued for 28 days. The animals (MM260 and MM242) were monitored for $CD4^+$ and $CD8^+$ T cell counts, viral loads in plasma, proviral DNA and $CD8^+$ T cell turnover.

MM260, the monkey with the high viral load showed a significant decline in $CD4^+$ but not $CD8^+$ T cell counts before HAART compared with the pre-infection level (598 ± 80 vs. 49 ± 16 per μl in mean $CD4^+$ count ± S.D., $P < 0.001$ determined by the Student's *t*-test, 288 ± 46 vs. 221 ± 81 per μl in mean $CD8^+$ count ± S.D., $P = 0.25$). $CD4^+$ and $CD8^+$ T cell counts

Table 1
Sensitivities of $SHIV_{89.6P}$ and $HIV\text{-}1_{LAI}$ to RTIs (AZT and 3TC) and PIs (LPV and RTV)

Virus	Cells	IC_{50} (μM) ± S.D.s[a]			
		AZT	3TC	LPV	RTV
$SHIV_{89.6P}$	M8166	0.007 ± 0.002	0.43 ± 0.0001	0.47 ± 0.09	0.44 ± 0.07
$HIV\text{-}1_{LAI}$	M8166	0.013 ± 0.001	0.31 ± 0.15	0.08 ± 0.01	0.03 ± 0.004

RTIs, reverse transcriptase inhibitors; AZT, zidovudine; 3TC, lamivudine. PIs, protease inhibitors; LPV, lopinavir; RTV, ritonavir.
[a] Data shown represent mean values (with standard deviations) derived from the result of two independent experiments conducted in duplicate. M8166 cells (5×10^3) were exposed to 100 $TCID_{50}$ of $SHIV_{89.6P}$ or $HIV\text{-}1_{LAI}$ caltured in the presence of various concentrations of RTIs or PIs, and IC_{50}s were determined using the MTT assay on day 7 of culture.

increased during and after treatment compared with the pre-HAART level (49 ± 16 vs. 99 ± 26 per μl in mean $CD4^+$ count ± S.D., $P = 0.002$, 221 ± 81 vs. 392 ± 108 per μl in mean $CD8^+$ count ± S.D., $P = 0.01$) (Fig. 1A). At week 38, when HAART was initiated, the plasma viral load in MM260 was 3.4×10^4 copies/ml, and the proviral DNA was 6.8×10^4 copies/μg DNA. After commencement of HAART, the viral RNA in the plasma declined to below the threshold of detection within 3 weeks post HAART. On the other hand, proviral DNA remained detectable under the treatment though a continuous decline in the level was observed at 9 weeks post HAART (Fig. 1B).

In the low viral load monkey, MM242, the $CD4^+$ cell numbers were maintained over 400 per μl before HAART but the macaque also showed a decline in $CD4^+$ but not $CD8^+$ T cell counts before HAART compared with the pre-infection level (2152 ± 542 vs.

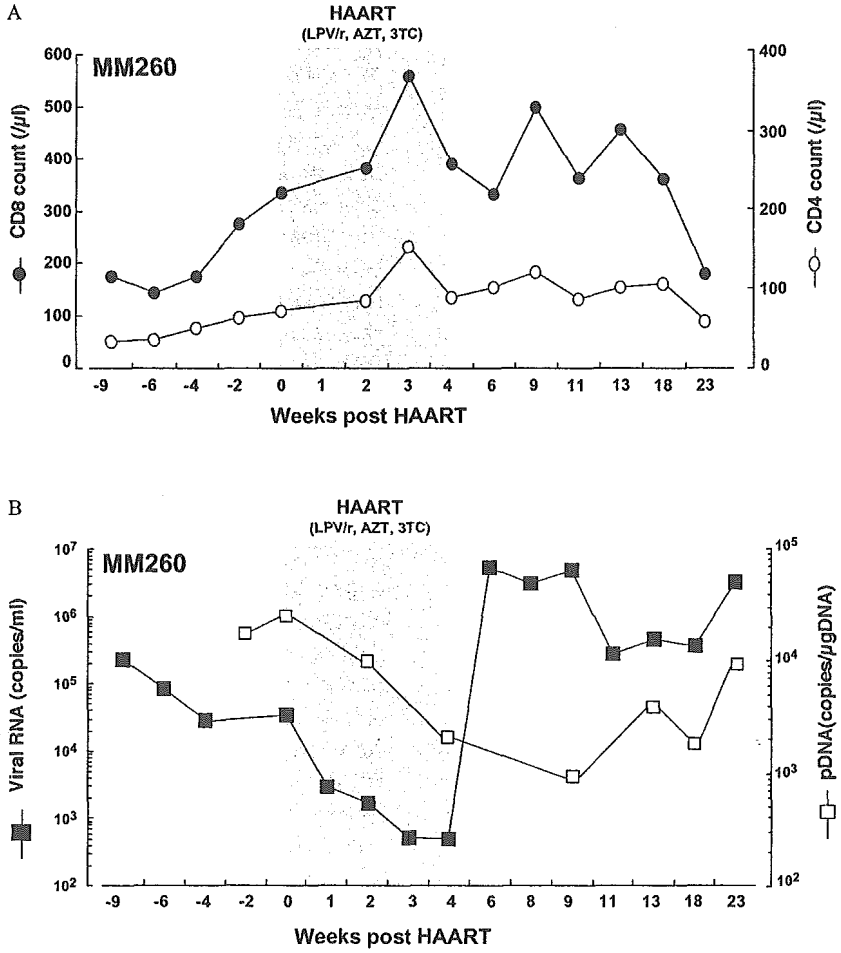

Fig. 1. Analyses of $SHIV_{89.6P}$-infected rhesus macaque MM260 treated with LPV/r, AZT and 3TC for 4 weeks by the oral route. $CD4^+$ and $CD8^+$ T cell counts (A), and plasma viral load and proviral DNA copy number (B) assessed within the peripheral blood are shown. The treatment period is shaded.

577±139 per μl in mean $CD4^+$ count±S.D., $P<0.001$, 761±248 vs. 447±188 per μl in mean $CD8^+$ count± S.D., $P=0.09$). However, there was no significant difference between pre- and after HAART in $CD4^+$ and $CD8^+$ T cell counts (577±139 vs. 569±180 per μl in mean $CD4^+$ count±S.D., $P=0.93$, 447±188 vs. 385±159 per μl in mean $CD8^+$ count±S.D., $P=0.52$) (Fig. 2A). The plasma viral load in MM242 was detectable at one point (9 weeks before HAART) before the treatment, and was never detected during and after treatment. The proviral DNAs in MM242 were also low (<300–1590 copies/μg DNA), and was maintained below the threshold of detection after the discontinuation of HAART (Fig. 2B).

3.3. Analysis of $CD8^+Ki67^+$ T cells in $SHIV_{89.6P}$-infected macaques with HAART

We determined Ki67-positive $CD8^+$ T cells in $SHIV_{89.6P}$-infected and uninfected monkeys using four-color flow cytometry analysis (Sachsenberg et al., 1998; Sodora et al., 2002). In the $SHIV_{89.6P}$-infected animal with a high viral load, MM260, growth fraction (percentage of Ki67) of $CD8^+$ T cells (10.98%) before HAART was higher than the value in the uninfected monkey (1.07%). The Ki67-positive $CD8^+$ T cells in MM260 were increasing during HAART, especially in the $CD45RA^-$ (CD8 memory) subset. After the discontinuation of HAART, the percentage of $CD8^+Ki67^+$ subset declined to the pre-treatment level (Fig. 3A and B). In MM242, the percentage of $CD8^+Ki67^+$ subset at 4 weeks before HAART was comparable to that of the uninfected monkey (0.83 vs. 0.85%). Ki67 levels were elevated after the treatment and were maintained at a high level until 18 weeks post HAART (7.95%). $CD8^+CD45RA^+Ki67^+$ T cells in MM242 increased after HAART, however, the $CD8^+CD45RA^-Ki67^+$ T cells were also increasing and overcame the percentage of $CD8^+CD45RA^+Ki67^+$ T cells by 13 weeks post HAART (Fig. 3C and D). We also determined Ki67 positivity in $CD8^+CD56^+$ T cells in MM242 at pre- and post-HAART. The percentages of $CD56^+Ki67^+$ were 0% and 0.05% in the $CD8^+$ T cell population at pre- (−3 weeks) and post- (22 weeks) HAART, respectively, using flow cytometry analysis. There

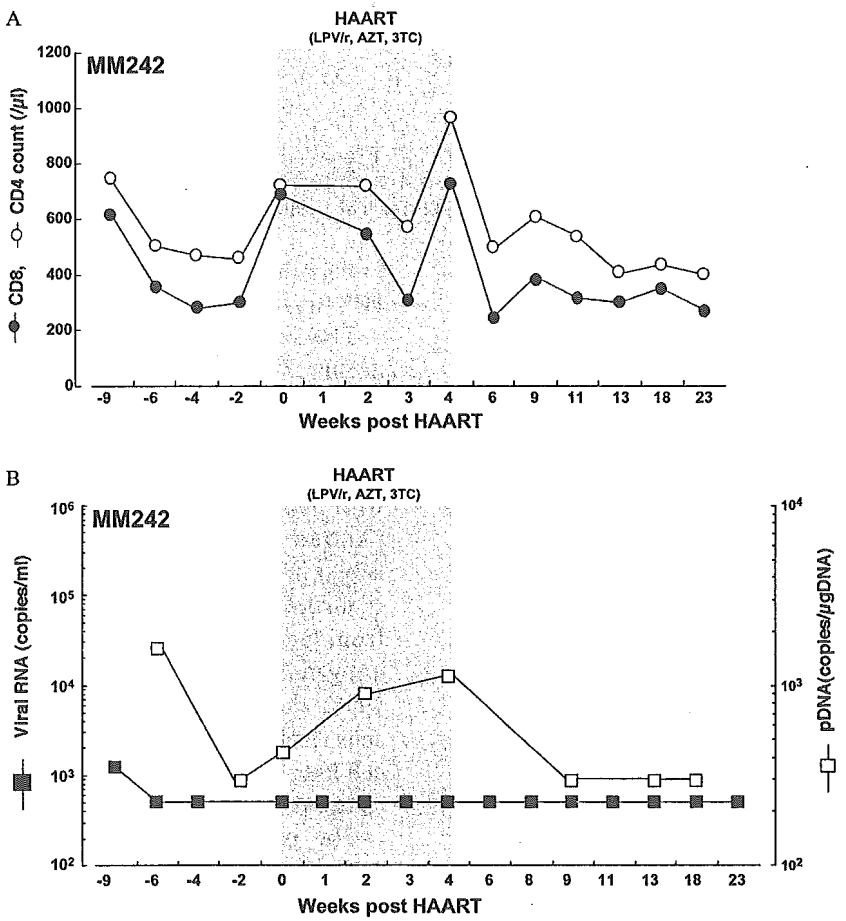

Fig. 2. Analyses of $SHIV_{89.6P}$-infected rhesus macaque MM242 treated with LPV/r, AZT and 3TC for 4 weeks by the oral route. $CD4^+$ and $CD8^+$ T cell counts (A), and plasma viral load and proviral DNA copy number (B) assessed within the peripheral blood are shown. The treatment period is shaded.

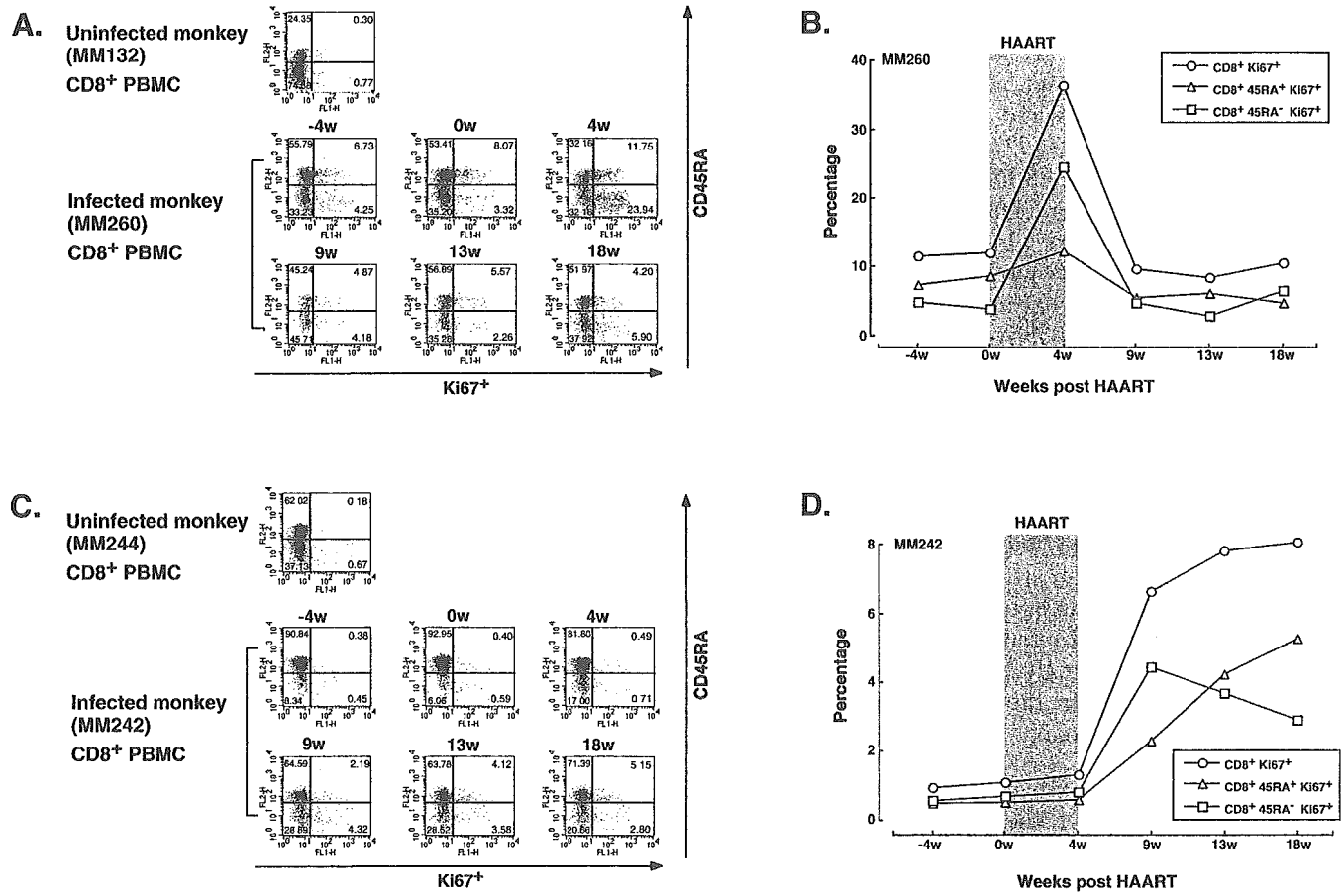

Fig. 3. Flow cytometry analysis of $CD8^+CD45RA^+$ cells stained with Ki-67. Expression of Ki-67 (percentage) in $CD8^+$ T cells of a control monkey and a $SHIV_{89.6P}$–infected monkey MM260 (A) and MM242 (C) at −4, 0, 4, 9, 13, 18 weeks post HAART. The percentage of cells expressing Ki-67 and CD45RA in $CD8^+$ T cells is depicted for MM260 (B) and MM242 (D). The treatment period is shaded.

seemed to be little contribution of $CD8^+$ NK cells in our data on $CD8^+Ki67^+$ T cells.

4. Discussion

This is apparently the first demonstration that the model of chronically $SHIV_{89.6P}$ infected-monkey with a therapeutic design recommended for humans by the oral route is feasible. The reduction of viral load and proviral DNA during the chronically infected stage was observed in treated animals together with the increase of CD4 and CD8 positive T lymphocyte subsets, especially memory T cells. Moreover, in both macaques, the percentages of $CD8^+Ki67^+$ cells increased during HAART, especially in the low viral load monkey (MM242) and the subset was maintained at a high percentage until 18 weeks post HAART. In CD4 positive T cells, $Ki67^+$ cells were also increased until 18 weeks post HAART in MM242 (data not shown). These results suggest that the oral treatment system in chronically infected-monkeys may prove to be a useful tool for monitoring immunological changes undergoing novel antiviral strategies with the usual anti-HIV treatment regimen.

The recent use of HAART has indicated that the decline of viral load in plasma and tissues generally results in an increase of T cell counts in peripheral blood (Autran et al., 1997; Evans et al., 1998; Mezzaroma et al., 1999; Pakker et al., 1998), which is often associated with improvement in clinical and immunological status (Autran et al., 1997; Evans et al., 1998). The mechanism(s) involved in such a peripheral T cell repopulation is unclear and may reflect the contribution of T cells from lymphoid tissues as a consequence of the reduced antigenic stimulation (Autran et al., 1997; Pakker et al., 1998), the capability for de novo production of naïve T cells (Hellerstein et al., 1999), and a decreased rate of T cell loss, which may reflect a reduced T cell susceptibility to apoptotic stimuli (Gougeon et al., 1999).

The issue of T lymphocyte turnover is central to understanding of HIV-1 pathogenesis (Antia and Halloran, 1996). Sachsenberg et al. estimated that HIV-1-infected individuals had a mean 6-fold increase in $CD8^+$T cell turnover, whereas the mean turnover of $CD4^+$T cells only increased by 2-fold (Sachsenberg et

al., 1998). The higher turnover of $CD8^+$T cells reflects the inversion of the $CD4^+/CD8^+$ ratio in HIV-1-infected patients (Chun et al., 2002; Margolick et al., 1995). In those studies, differences in $CD4^+$ and $CD8^+$T cell turnover also depend on stage of the disease, as defined by $CD4^+$ T cell counts.

$CD8^+$ T cell counts and the percentage of $CD8^+CD45RA^-$ (memory) T cells in both chronically infected macaques increased after oral route treatment. These findings were usually seen in clinical cases at the beginning of HAART (Autran et al., 1997; Badley et al., 1999; Pakker et al., 1998). However, the majority of $CD8^+$ memory cells increased following HAART was not considered as HIV-specific T cells. Because levels of HIV-specific effect CTL in treatment individuals fell (median half-life, 45 days) while viral RNA remained undetectable (Ogg et al., 1999). It is conceivable that following HAART reduction of apoptosis in $CD8^+$ memory cells may lead to an increase in the population. Our finding in infected monkeys with HAART was very similar to the kinetic of $CD8^+$ T cells after treatment of humans. The experiment presented in this report may provide an animal model of the phenomenon observed in HIV infected patients. Further analysis of repopulated $CD8^+$ T cells would be of interest because HIV-1 specific $CD8^+$ T cells during chronic infection in humans are enriched in cells of the $CD28^-CD27^+$ phenotype that proliferate but do have reduced CTL activity (Appay et al., 2002). Whether or not the proliferating $CD8^+$ T cells in our macaques given HAART are cells of this phenotype will need to be determined.

The plasma HIV-1 RNA is widely considered to be a direct indicator of the overall level of HIV-1 expression in infected individuals. However, it was reported that the concentration of HIV-1 DNA in PBMC complements the HIV-1 RNA load in plasma in predicting the clinical outcome of HIV-1 disease (Kostrikis et al., 2002). In our findings, especially in MM242 with a low plasma $SHIV_{89.6P}$ RNA load, the proviral DNA also may be an indicator of residual replication when plasma RNA loads were undetectable as seen in HIV-1 infected patients (Kostrikis et al., 2002; O'Doherty et al., 2002).

These monkey model given antiviral drugs by the oral route will enable the investigation of immunological changes during novel drug testing and also antiviral strategies combined with HAART.

Acknowledgements

We thank K. Yoshida and N. Shirai for excellent technical assistance and Dr A. Koito for helpful comments on the manuscript. This work was supported in part by Research for Scientific Research Grant of the Japan Society for the Promotion of Science (#14021099), a Grant-in-Aid for Scientific Research (Priority Areas) from the Ministry of Education, Culture, Sports, Science, and Technology of Japan (Monbu-Kagakusho)(#14570422).

References

Antia, R., Halloran, M.E., 1996. Recent developments in theories of pathogenesis of AIDS. Trends Microbiol. 4 (7), 282–285.

Appay, V., Dunbar, P.R., Callan, M., Klenerman, P., Gillespie, G.M., Papagno, L., Ogg, G.S., King, A., Lechner, F., Spina, C.A., Little, S., Havlir, D.V., Richman, D.D., Gruener, N., Pape, G., Waters, A., Easterbrook, P., Salio, M., Cerundolo, V., McMichael, A.J., Rowland-Jones, S.L., 2002. Memory $CD8^+$ T cells vary in differentiation phenotype in different persistent virus infections. Nat. Med. 8 (4), 379–385.

Autran, B., Carcelain, G., Li, T.S., Blanc, C., Mathez, D., Tubiana, R., Katlama, C., Debre, P., Leibowitch, J., 1997. Positive effects of combined antiretroviral therapy on $CD4^+$ T cell homeostasis and function in advanced HIV disease. Science 277 (5322), 112–116.

Badley, A.D., Parato, K., Cameron, D.W., Kravcik, S., Phenix, B.N., Ashby, D., Kumar, A., Lynch, D.H., Tschopp, J., Angel, J.B., 1999. Dynamic correlation of apoptosis and immune activation during treatment of HIV infection. Cell Death Differ. 6 (5), 420–432.

Carrillo, A., Stewart, K.D., Sham, H.L., Norbeck, D.W., Kohlbrenner, W.E., Leonard, J.M., Kempf, D.J., Molla, A., 1998. In vitro selection and characterization of human immunodeficiency virus type 1 variants with increased resistance to ABT-378, a novel protease inhibitor. J. Virol. 72 (9), 7532–7541.

Chun, T.W., Justement, J.S., Pandya, P., Hallahan, C.W., McLaughlin, M., Liu, S., Ehler, L.A., Kovacs, C., Fauci, A.S., 2002. Relationship between the size of the human immunodeficiency virus type 1 (HIV-1) reservoir in peripheral blood $CD4^+$ T cells and $CD4^+$:$CD8^+$ T cell ratios in aviremic HIV-1-infected individuals receiving long-term highly active antiretroviral therapy. J. Infect. Dis. 185 (11), 1672–1676.

Clapham, P.R., Weiss, R.A., Dalgleish, A.G., Exley, M., Whitby, D., Hogg, N., 1987. Human immunodeficiency virus infection of monocytic and T-lymphocytic cells: receptor modulation and differentiation induced by phorbol ester. Virology 158 (1), 44–51.

Clavel, F., Guetard, D., Brun-vezinet, F., Chamaret, S., Rey, M.A., Santos-ferreira, M.O., Laurent, A.G., Dauguet, C., Katlama, C., Rouzioux, C., 1986. Isolation of a new human retrovirus from West African patients with AIDS. Science 233 (4761), 343–346.

Endo, Y., Igarashi, T., Nishimura, Y., Buckler, C., Buckler-White, A., Plishka, R., Dimitrov, D.S., Martin, M.A., 2000. Short- and long-term clinical outcomes in rhesus monkeys inoculated with a highly pathogenic chimeric simian/human immunodeficiency virus. J. Virol. 74 (15), 6935–6945.

Enose, Y., Ui, M., Miyake, A., Suzuki, H., Uesaka, H., Kuwata, T., Kunisawa, J., Kiyono, H., Takahashi, H., Miura, T., Hayami, M., 2002. Protection by intranasal immunization of a nef-deleted, nonpathogenic SHIV against intravaginal challenge with a heterologous pathogenic SHIV. Virology 298 (2), 306–316.

Evans, T.G., Bonnez, W., Soucier, H.R., Fitzgerald, T., Gibbons, D.C., Reichman, R.C., 1998. Highly active antiretroviral therapy results in a decrease in $CD8^+$ T cell activation and preferential reconstitution of the peripheral $CD4^+$ T cell population with memory rather than naive cells. Antiviral Res. 39 (3), 163–173.

Gougeon, M.L., Lecoeur, H., Sasaki, Y., 1999. Apoptosis and the CD95 system in HIV disease: impact of highly active anti-retroviral therapy (HAART). Immunol. Lett. 66 (1–3), 97–103.

Haigwood, N.L., 1999. Progress and challenges in therapies for AIDS in nonhuman primate models. J. Med. Primatol. 28 (4–5), 154–163.

Hellerstein, M., Hanley, M.B., Cesar, D., Siler, S., Papageorgopoulos, C., Wieder, E., Schmidt, D., Hoh, R., Neese, R., Macallan, D., Deeks, S., McCune, J.M., 1999. Directly measured kinetics of circulating T lymphocytes in normal and HIV-1-infected humans. Nat. Med. 5 (1), 83–89.

Igarashi, T., Brown, C.R., Endo, Y., Buckler-White, A., Plishka, R., Bischofberger, N., Hirsch, V., Martin, M.A., 2001. Macrophage are the principal reservoir and sustain high virus loads in rhesus macaques after the depletion of $CD4^+$ T cells by a highly pathogenic simian immunodeficiency virus/HIV type 1 chimera (SHIV): implications for HIV-1 infections of humans. Proc. Natl. Acad. Sci. USA 98 (2), 658–663.

Kimura, T., Yoshimura, K., Nishihara, K., Maeda, Y., Matsumi, S., Koito, A., Matsushita, S., 2002. Reconstitution of spontaneous neutralizing antibody response against autologous human immunodeficiency virus during highly active antiretroviral therapy. J. Infect. Dis. 185 (1), 53–60.

Kostrikis, L.G., Touloumi, G., Karanicolas, R., Pantazis, N., Anastassopoulou, C., Karafoulidou, A., Goedert, J.J., Hatzakis, A., 2002. Quantitation of human immunodeficiency virus type 1 DNA forms with the second template switch in peripheral blood cells predicts disease progression independently of plasma RNA load. J. Virol. 76 (20), 10099–10108.

Le Grand, R., Clayette, P., Noack, O., Vaslin, B., Theodoro, F., Michel, G., Roques, P., Dormont, D., 1994. An animal model for antilentiviral therapy: effect of zidovudine on viral load during acute infection after exposure of macaques to simian immunodeficiency virus. AIDS Res. Hum. Retroviruses 10 (10), 1279–1287.

Le Grand, R., Vaslin, B., Larghero, J., Neidez, O., Thiebot, H., Sellier, P., Clayette, P., Dereuddre-Bosquet, N., Dormont, D., 2000. Post-exposure prophylaxis with highly active antiretroviral therapy could not protect macaques from infection with SIV/HIV chimera. AIDS 14 (12), 1864–1866.

Le Grand, R., Vaslin, B., Benlhassan, K., Thiebot, H., Dereuddre-Bosquet, N., Clayette, P., Dormont, D., 2002. Post-exposure prophylaxis with HAART in macaques exposed to pathogenic SIV or SHIV. XIV International AIDS Conference.

Li, J., Lord, C.I., Haseltine, W., Letvin, N.L., Sodroski, J., 1992. Infection of cynomolgus monkeys with a chimeric HIV-1/SIVmac virus that expresses the HIV-1 envelope glycoproteins. J. Acquired Immune Defic. Syndr. 5 (7), 639–646.

Maeda, K., Yoshimura, K., Shibayama, S., Habashita, H., Tada, H., Sagawa, K., Miyakawa, T., Aoki, M., Fukushima, D., Mitsuya, H., 2001. Novel low molecular weight spirodiketopiperazine derivatives potently inhibit R5 HIV-1 infection through their antagonistic effects on CCR5. J. Biol. Chem. 276 (37), 35194–35200.

Margolick, J.B., Munoz, A., Donnenberg, A.D., Park, L.P., Galai, N., Giorgi, J.V., O'Gorman, M.R., Ferbas, J., 1995. Failure of T-cell homeostasis preceding AIDS in HIV-1 infection. The Multicenter AIDS Cohort Study. Nat. Med. 1 (7), 674–680.

Mezzaroma, I., Carlesimo, M., Pinter, E., Alario, C., Sacco, G., Muratori, D.S., Bernardi, M.L., Paganelli, R., Aiuti, F., 1999. Long-term evaluation of T-cell subsets and T-cell function after HAART in advanced stage HIV-1 disease. AIDS 13 (10), 1187–1193.

Nath, B.M., Schumann, K.E., Boyer, J.D., 2000. The chimpanzee and other non-human-primate models in HIV-1 vaccine research. Trends Microbiol. 8 (9), 426–431.

Nathanson, N., Hirsch, V.M., Mathieson, B.J., 1999. The role of nonhuman primates in the development of an AIDS vaccine. AIDS 13 (Suppl. A), S113–S120.

O'Doherty, U., Swiggard, W.J., Jeyakumar, D., McGain, D., Malim, M.H., 2002. A sensitive, quantitative assay for human immunodeficiency virus type 1 integration. J. Virol. 76 (21), 10942–10950.

Ogg, G.S., Jin, X., Bonhoeffer, S., Moss, P., Nowak, M.A., Monard, S., Segal, J.P., Cao, Y., Rowland-Jones, S.L., Hurley, A., Markowitz, M., Ho, D.D., McMichael, A.J., Nixon, D.F., 1999. Decay kinetics of human immunodeficiency virus-specific effector cytotoxic T lymphocytes after combination antiretroviral therapy. J. Virol. 73 (1), 797–800.

Pakker, N.G., Notermans, D.W., de Boer, R.J., Roos, M.T., de Wolf, F., Hill, A., Leonard, J.M., Danner, S.A., Miedema, F., Schellekens, P.T., 1998. Biphasic kinetics of peripheral blood T cells after triple combination therapy in HIV-1 infection: a composite of redistribution and proliferation. Nat. Med. 4 (2), 208–214.

Reimann, K.A., Li, J.T., Veazey, R., Halloran, M., Park, I.W., Karlsson, G.B., Sodroski, J., Letvin, N.L., 1996a. A chimeric simian/human immunodeficiency virus expressing a primary patient human immunodeficiency virus type 1 isolate env causes an AIDS- like disease after in vivo passage in rhesus monkeys. J. Virol. 70 (10), 6922–6928.

Reimann, K.A., Li, J.T., Voss, G., Lekutis, C., Tenner-Racz, K., Racz, P., Lin, W., Montefiori, D.C., Lee-Parritz, D.E., Lu, Y., Collman, R.G., Sodroski, J., Letvin, N.L., 1996b. An env gene derived from a primary human immunodeficiency virus type 1 isolate confers high in vivo replicative capacity to a chimeric simian/human immunodeficiency virus in rhesus monkeys. J. Virol. 70 (5), 3198–3206.

Sachsenberg, N., Perelson, A.S., Yerly, S., Schockmel, G.A., Leduc, D., Hirschel, B., Perrin, L., 1998. Turnover of $CD4^+$ and $CD8^+$ T lymphocytes in HIV-1 infection as measured by Ki-67 antigen. J. Exp. Med. 187 (8), 1295–1303.

Sodora, D.L., Milush, J.M., Ware, F., Wozniakowski, A., Montgomery, L., McClure, H.M., Lackner, A.A., Marthas, M., Hirsch, V., Johnson, R.P., Douek, D.C., Koup, R.A., 2002. Decreased levels of recent thymic emigrants in peripheral blood of simian immunodeficiency virus-infected macaques correlate with alterations within the thymus. J. Virol. 76 (19), 9981–9990.

Tang, Y., Villinger, F., Staprans, S.I., Amara, R.R., Smith, J.M., Herndon, J.G., Robinson, H.L., 2002. Slowly declining levels of viral RNA and DNA in DNA/recombinant modified vaccinia virus Ankara-vaccinated macaques with controlled simian-human immunodeficiency virus SHIV-89.6P challenges. J. Virol. 76 (20), 10147–10154.

Thiebot, H., Louache, F., Vaslin, B., de Revel, T., Neildez, O., Larghero, J., Vainchenker, W., Dormont, D., Le Grand, R., 2001. Early and persistent bone marrow hematopoiesis defect in simian/human immunodeficiency virus-infected macaques despite efficient reduction of viremia by highly active antiretroviral therapy during primary infection. J. Virol. 75 (23), 11594–11602.

Ui, M., Kuwata, T., Igarashi, T., Ibuki, K., Miyazaki, Y., Kozyrev, I.L., Enose, Y., Shimada, T., Uesaka, H., Yamamoto, H., Miura, T., Hayami, M., 1999. Protection of macaques against a SHIV with a homologous HIV-1 Env and a pathogenic SHIV-89.6P with a heterologous Env by vaccination with multiple gene-deleted SHIVs. Virology 265 (2), 252–263.

Yoshimura, K., Kato, R., Yusa, K., Kavlick, M.F., Maroun, V., Nguyen, A., Mimoto, T., Ueno, T., Shintani, M., Falloon, J., Masur, H., Hayashi, H., Erickson, J., Mitsuya, H., 1999. JE-2147: a dipeptide protease inhibitor (PI) that potently inhibits multi-PI-resistant HIV-1. Proc. Natl. Acad. Sci. USA 96 (15), 8675–8680.

NOTE *Virology*

Infection of a Chimeric Simian and Human Immunodeficiency Virus with CCR5-Specific HIV-1 Envelope to Rhesus Macaques

Yoshimi ENOSE[1)], Ariko MIYAKE[1)], Eiji IDO[1)] and Masanori HAYAMI[1)]

[1)]*Institute for Virus Research, Kyoto University, 53 Kawahara-cho, Shogoin, Sakyo-ku, Kyoto 606–8507, Japan*

(Received 21 June 2002/Accepted 11 November 2002)

ABSTRACT. Human immunodeficiency virus (HIV) infects lymphocytes and macrophages via CD4 and chemokine receptors. In this study, the infectivity of a chimeric simian and human immunodeficiency virus (SHIV) having a CCR5-specific HIV-1 envelope gene was examined. A SHIV strain termed SHIV-JRFL could enter cells via CD4 with a chemokine receptor CCR5, not CXCR4, and the viral replication was suppressed by recombinant human RANTES, one of β-chemokines. The intravenous inoculation of SHIV-JRFL into two rhesus macaques resulted in a systemic infection, though it was rather weak. During the early infection, the production of RANTES from Con A-stimulated PBMCs of the infected monkeys increased. These results suggested that β-chemokine has the potential to limit the infectivity of an R5-type SHIV.

KEY WORDS: CCR5, RANTES, SHIV.

J. Vet. Med. Sci. 65(2): 283–286, 2003

Human immunodeficiency virus (HIV) infects lymphocytes and macrophages and is biologically classified into two main groups, macrophage-tropic (M-tropic) and T cell-tropic (T-tropic) strains. The entry of HIV-1 into target cells is mediated by the interaction between the viral envelope glycoprotein and a cellular receptor complex consisting of CD4 and one or more members of the CC or CXC chemokine receptor family [6, 8–10, 12]. Berger *et al.* [3] have proposed defining the phenotype of HIV-1 isolates based on the usage of co-receptors. The biological phenotype of a virus can change during disease progression in HIV-infected patients. M-tropic viruses, which are known to use CCR5 as a co-receptor, predominate in early infection, while T-tropic viruses that use CXCR4 appear as the disease progress [7]. Therefore, delineating the whole infection process of a CCR5-type virus (R5-virus) is important for understanding viral transmission and progression of the disease to AIDS.

Chimeric simian and human immunodeficiency viruses (SHIVs) which have an HIV-1 envelope gene (*env*) inserted into the SIV genome were constructed in several laboratories, and used to infect macaque monkeys [14, 18, 20, 25, 26]. SHIV generally showed the phenotype and the usage of co-receptors similar to those of the parental HIV-1 *env* that was inserted to the SHIV [5, 14–16, 21]. Therefore, the co-receptor usage and the biological property of the HIV-1 Env can be analyzed *in vivo* by using the SHIV. In this study, to examine the infectivity of an R5-type SHIV in rhesus macaques, we inoculated such a strain termed SHIV-JRFL to rhesus macaques and analyzed its viral infectivity.

SHIV-JRFL was constructed by insertion of a StuI - BglII fragment of the HIV-1 JRFL env (nucleotides 6139-6910 in HIV-1 strain JRFL, GenBank accession number: U63632) in SHIV-NM-3rN [4]. This chimeric virus could efficiently replicate in human PBMCs and macrophages, and has the same cell tropism characteristics as HIV-1 JRFL, which can also replicate in human PBMCs and macrophages [19, 24]. However, SHIV-JRFL could not replicate in rhesus macaque macrophages, but could replicate in rhesus PBMCs [4]. In this study, we first determined the co-receptor usage of SHIV-JRFL and the parental T-tropic virus, SHIV-NM-3rN, by using GHOST cells transfected with either CXCR4 or CCR5 and a reporter construct encoding enhanced green fluorescent protein (GFP). These cell lines were obtained through the NIAID/NIH AIDS Research and Reference Reagent Program and were contributed by Vincent N. KewalRamani and Dan R. Littman [23]. The viral stock was prepared from the culture supernatant of a cynomolgus macaque T cell line, HSC-F, infected with SHIV-JRFL or SHIV-NM-3rN, and the 50% tissue culture infectious dose ($TCID_{50}$) of the viral stock was determined in HSC-F. After infection to GHOST cell lines with undiluted virus stocks, GFP expression was detected by flow cytometry at 3 days post infection. As the results, SHIV-JRFL used CD4 and CCR5, but not CXCR4, to enter the cells, while SHIV-NM-3rN used CD4 and CXCR4, but not CCR5 (Table 1). These co-receptor usages of SHIV-JRFL and SHIV-NM-3rN were the same as those of HIV-1 JRFL and HIV-1 NL432, respectively [27], showing that HIV-1 Env region inserted into SHIV determined the co-receptor usage of the virus strain. Thus, SHIV-JRFL could infect the PBMC using CD4 and CCR5, because rhesus macaque

Table 1. Coreceptor usage of SHIV-JRFL and SHIV-NM-3rN

Virus	GHOST cell	
	CXCR4	CCR5
SHIV-JRFL	–	+
SHIV-NM-3rN	++	–

Coreceptor specific GFP expression was detected by flow cytometry. The detected value was represented as <1% (–), 2–5% (+) and >5% (++).

PBMC expressed CD4 and both chemokine receptors. Although rhesus macaque macrophages also expressed CD4 and CCR5, the restriction of SHIV-JRFL to rhesus macaque macrophages might be ascribed to other cellular reasons, such as low expression of CD4, rather than viral factors [2, 22].

To assess the role of the HIV co-receptor CCR5 in SHIV-JRFL replication in macaque T cells, we next determined whether RANTES, one of the ligands of CCR5, could block the entry of SHIV-JRFL into rhesus macaque PBMCs. One day before virus infection, recombinant human RANTES (Peprotech, Inc., Rockey Hill, N.J.) was added to the culture of Con A-stimulated rhesus macaque PBMCs at concentration of 0, 10, 20 and 100 *ng/ml*. Virus stock of SHIV-JRFL or SHIV-NM-3rN was added to each well at a moi of 0.01. The culture supernatants were collected every three days and viral replication was monitored by reverse transcriptase (RT) activity, as described previously [11]. The viral inhibition by RANTES was compared at 16 days post infection, at the peak value of each viral replication in rhesus macaque PBMCs. The inhibitory effect of RANTES was expressed as R/Ro, where R and Ro are the viral replication in the presence and absence of RANTES, respectively. We found that RANTES clearly inhibited SHIV-JRFL in rhesus macaque PBMC culture in a dose-dependent manner, while it did not inhibit SHIV-NM-3rN (Fig. 1). RANTES was able to control replication of the R5 virus, but not the X4 virus, in rhesus macaque PBMC culture, indicating that SHIV-JRFL is an R5 type virus.

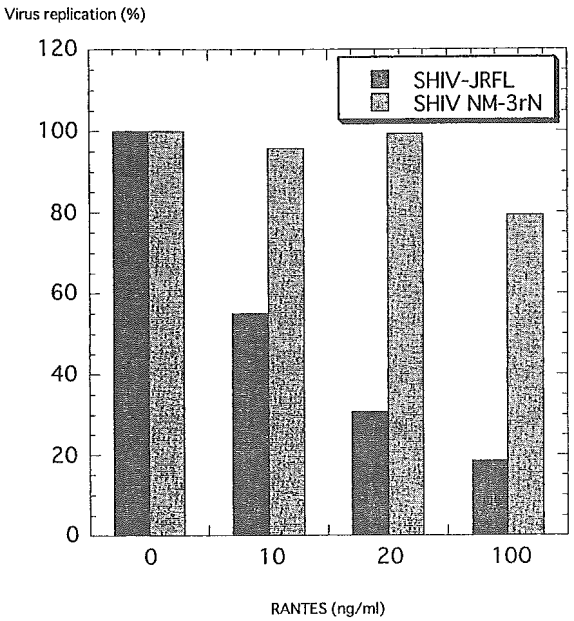

Fig. 1. Inhibition of replication of SHIV-JRFL and SHIV-NM-3rN by recombinant human RANTES in rhesus macaque PBMCs. Virus replication was measured by reverse transcriptase activity of the culture supernatant 16 days post infection. Values are expressed as the percentages of the viral replication compared with the value in the absence of recombinant RANTES.

To examine the infectivity of SHIV-JRFL *in vivo*, two rhesus macaques (*Macaca Mulatta*) (MM226 and MM227), about four kilograms in weight, were anesthetized by intramuscular injection of ketamine chloride and intravenously inoculated with 1×10^4 $TCID_{50}$ of SHIV-JRFL. Throughout the experimental period, the monkeys were housed in accordance with regulations approved by the Institutional Animal Care and Use Committee of the Institute for Virus Research, Kyoto University. The blood was periodically collected from all monkeys. PBMCs were separated from heparinized blood by Percoll gradient and plasma samples were frozen at –80°C until analysis. The viral infection was assessed by virus recovery from PBMCs, detection of proviral DNAs in PBMCs and viral RNA loads in plasma. Infectious viruses were recovered by coculture of 1×10^6 cells of CD8-depleted PBMCs with 1×10^6 cells of HSC-F for at least one month. Depletion of $CD8^+$ cells was performed as previously described [11]. Virus recovery was confirmed by the appearance of syncytium formation and RT activity in the culture supernatants. Proviral DNAs were detected by nested PCR for the amplification of HIV-1 V3 region (359 bp) as previously described [17]. Cellular DNAs were extracted from PBMCs of the inoculated monkeys with a DNeasy Tissue Kit (QIAGEN, Germany) and added to a mixture including AmpliTaq DNA polymerase (Perkin Elmer, Norwalk, CT). Table 2 summarizes the results of virological and immunological status of SHIV-JRFL-inoculated monkeys. The proviral DNAs in PBMCs were first detected at 1 week post inoculation (wpi) in MM207 and at 2 wpi in MM206, and persistently detected in both monkeys

Table 2. Virological and immunological status of SHIV-JRFL-inoculated monkeys

Monkey		0	1	2	3	4[b)]	8	12	20	26	40	52[b)]
MM226	Proviral DNA	–	–	+	+	+(+)	+	+	+	–	+	–(+)
	Virus isolation[a)]	–	–	+	–	–(+)	–	–	–	–	–	–
	Antibody response	–	–	–	–	–	512	1024	2048	4096	2048	2048
MM227	Proviral DNA	–	–	–	+	+(+)	+	+	+	+	–	+ (+)
	Virus isolation[a)]	–	–	–	+	–(+)	–	–	–	–	–	–
	Antibody response	–	–	–	–	128	2048	4096	16384	16384	16384	16384

a) Virus isolation was performed by coculture with monkey T cell lines, HSC-F, and $CD8^+$ cells-depleted PBMCs.
b) The inguinal LNs were collected from each monkey at 4 and 52 weeks post inoculation by biopsy. The detection of proviral DNAs in LNs was represented in parentheses.

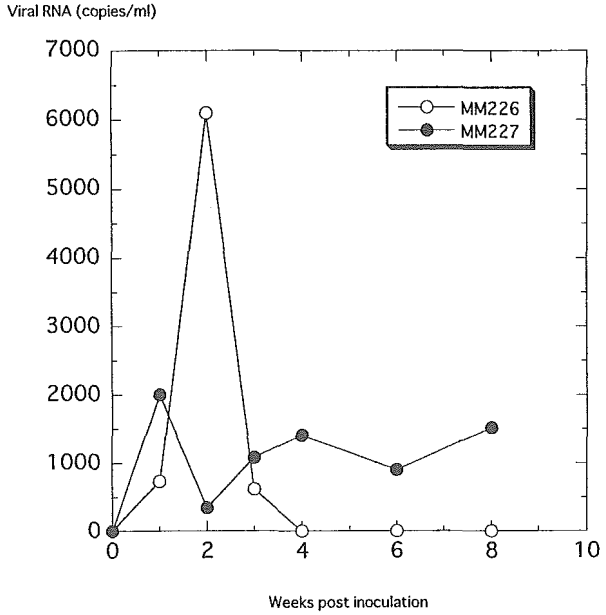

Fig. 2. Plasma viral RNA loads in two SHIV-JRFL-infected monkeys (MM226 and MM227). Total RNAs were prepared from plasma of each monkey and RT-PCR was performed using SIV gag specific primers. The amplified PCR products were quantified in real time using SIV gag specific labeled probe [28].

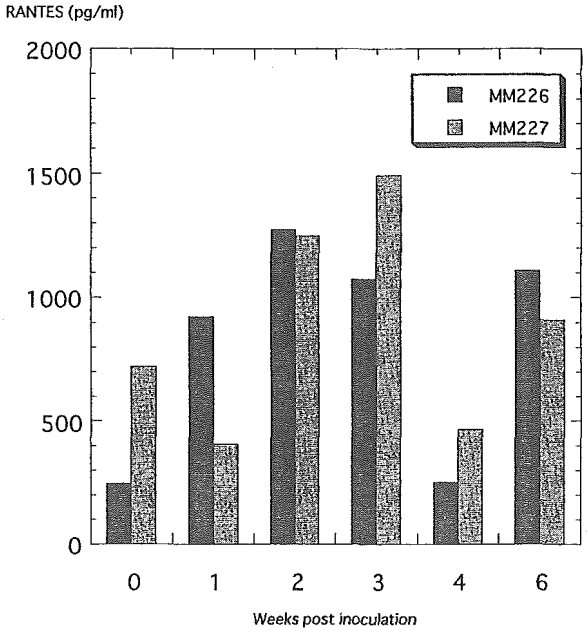

Fig. 3. Production of RANTES by PBMCs obtained from SHIV-JRFL-infected monkeys (MM226 and MM227). RANTES was assayed in the supernatants from Con A-stimulated PBMCs by ELISA. Data show the concentrations of RANTES in each culture supernatant.

till 52 wpi. The infectious viruses were isolated from PBMCs early after infection or from the inguinal lymph nodes obtained at 4 wpi by biopsy. HIV-1 Env-specific antibodies gradually increased in the plasma of both monkeys and were detected at serial dilutions of 4096 or 16384 by the particle agglutination method (Serodia HIV-1/2, Fujirebio Inc., Tokyo, Japan). Thus, it is obvious that the infection of SHIV-JRFL to rhesus macaques was achieved.

Viral RNA loads in plasma were also determined by quantitative RT-PCR as previously described [28]. The viral RNA of SHIV-JRFL was detected in the plasma of both monkeys and the viral RNA loads transiently increased in the early phase of infection (Fig. 2). However, the peak value of viral RNA load of SHIV-JRFL in the plasma at 2 wpi was far lower approximately 0.1% than that of SHIV-NM-3rN [28].

To examine the reason why the infectivity of SHIV-JRFL to rhesus macaque monkeys were weak, we analyzed the RANTES production in PBMCs of the infected monkeys early after infection. The PBMCs (2×10^5 cells) were stimulated in RPMI medium containing 1 μg/ml of Con A and cultured in RPMI medium containing recombinant human IL-2 for three days. The concentration of RANTES in the culture supernatants was measured using a human RANTES ELISA kit (R & D Systems, Minneapolis, Minn), which is known to cross-react with rhesus chemokine [1, 13]. As shown in Fig. 3, RANTES was detected in the culture supernatants in Con A-stimulated PBMCs of both monkeys after SHIV-JRFL infection although it was not detected in unstimulated PBMCs (data not shown). In the PBMCs of both monkeys, RANTES production gradually increased and peaked at two or three wpi. Thus, SHIV-JRFL transiently induced the production of RANTES early after infection, which might block viral infection, especially an R5 type-virus infection. These results confirmed previous reports that infection of macaques with a live -attenuated SIV induced the production of β-chemokines [1, 13].

Although SHIV utilizing CXCR4 or both CXCR4 and CCR5 were examined well about the disease progression and as challenge virus against vaccine candidate, little is examined about R5 type-SHIV. Recently, more pathogenic R5 type-SHIV was reported to infect into rhesus macaques by both intravenous and mucosal routes and induce simian AIDS [5, 15, 16]. $SHIV_{SF162P3}$ was generated from non-pathogenic R5 type-SHIV, $SHIV_{SF162}$ molecular clone, by sequential blood-bone marrow transfusions into rhesus macaques [15, 16]. Importantly, *in vivo* adaptation to a pathogenic variant of the parental virus was required to obtain the pathogenicities of SHIV. To generate more pathogenic SHIV-JRFL variant, we should attempt *in vivo* adaptation of the virus enough to overcome host defense against the virus infection in rhesus macaques.

HIV-1 infects various cells, expressing not only CXCR4 but also CCR5, of infected individuals. Therefore, both X4 type-SHIV and R5 type-SHIV should be developed and characterized to mimic natural HIV-1 infection using macaque model. Further studies are necessary to understand the pathogenicity of each SHIV *in vivo*.

ACKNOWLEDGMENTS. This work was supported by a Health Sciences Research Grant from the Ministry of Health, Labour and Welfare, Japan, and a Grant-in-Aid for Scientific Research from the Ministry of Education and Science, Japan. Y. E. is recipient of a Research Fellowship of the Japan Society for the Promotion of Science for Young Scientists.

REFERENCES

1. Ahmed, R. K., Nilsson, C., Wang, Y., Lehner, T., Biberfeld, G. and Thorstensson, R. 1999. *J. Gen. Virol.* **80**: 1569–1574.
2. Bannert, N., Schenten, D., Craig, S. and Sodroski, J. 2000. *J. Virol.* **74**: 10984–10993.
3. Berger, E. A., Doms, R. W., Fenyo, E. M., Korber, B. T., Littman, D. R., Moore, J. P., Sattentau, Q. J., Schuitemaker, H., Sodroski, J. and Weiss, R. A. 1998. *Nature (Lond.)* **391**: 240.
4. Chen, J., Ido, E., Jin, M., Kuwata, T., Igarashi, T., Mizuno, A., Koyanagi, Y. and Hayami, M. 1998. *J. Gen. Virol.* **79**: 741–745.
5. Chen, Z., Huang, Y., Zhao, X., Skulsky, E., Lin, D., Ip, J., Gettie, A. and Ho, D. D. 2000. *J. Virol.* **74**: 6501–6510.
6. Choe, H., Farzan, M., Sun, Y., Sullivan, N., Rollins, B., Ponath, P. D., Wu, L., Mackay, C. R., LaRosa, G., Newman, W., Gerard, N., Gerard, C. and Sodroski, J. 1996. *Cell* **85**: 1135–1148.
7. Connor, R. I., Sheridan, K. E., Ceradini, D., Choe, S. and Landau, N. R. 1997. *J. Exp. Med.* **185**: 621–628.
8. Deng, H., Liu, R., Ellmeier, W., Choe, S., Unutmaz, D., Burkhart, M., Di Marzio, P., Marmon, S., Sutton, R. E., Hill, C. M., Davis, C. B., Peiper, S. C., Schall, T. J., Littman, D. R. and Landau, N. R. 1996. *Nature (Lond).* **381**: 661–666.
9. Doranz, B. J., Rucker, J., Yi, Y., Smyth, R. J., Samson, M., Peiper, S. C., Parmentier, M., Collman, R. G. and Doms, R. W. 1996. *Cell* **85**: 1149–1158.
10. Dragic, T., Litwin, V., Allaway, G. P., Martin, S. R., Huang, Y., Nagashima, K. A., Cayanan, C., Maddon, P. J., Koup, R. A., Moore, J. P. and Paxton, W. A. 1996. *Nature (Lond.)* **381**: 667–673.
11. Enose, Y., Ibuki, K., Tamaru, K., Ui, M., Kuwata, T., Shimada, T. and Hayami, M. 1999. *J. Gen. Virol.* **80**: 847–855.
12. Feng, Y., Broder, C. C., Kennedy, P. E. and Berger, E. A. 1996. *Science* **272**: 872–877.
13. Gauduin, M. C., Glickman, R. L., Ahmad, S., Yilma, T. and Johnson, R. P. 1999. *Proc. Natl. Acad. Sci. U. S. A.* **96**: 14031–14036.
14. Harouse, J. M., Tan, R. C., Gettie, A., Dailey, P., Marx, P. A., Luciw, P. A. and Cheng-Mayer, C. 1998. *Virology* **248**: 95–107.
15. Harouse, J. M., Gettie, A., Tan, R. C., Blanchard, J. and Cheng-Mayer, C. 1999. *Science* **284**: 816–819.
16. Harouse, J. M., Gettie, A., Eshetu, T., Tan, R. C., Bohm, R., Blanchard, J., Baskin, G. and Cheng-Mayer, C. 2001. *J. Virol.* **75**: 1990–1995.
17. Igarashi, T., Kuwata, T., Takehisa, J., Ibuki, K., Shibata, R., Mukai, R., Komatsu, T., Adachi, A., Ido, E. and Hayami, M. 1996. *J. Gen. Virol.* **77**: 1649–1658.
18. Joag, S. V., Li, Z., Foresman, L., Stephens, E. B., Zhao, L. J., Adany, I., Pinson, D. M., McClure, H. M. and Narayan, O. 1996. *J. Virol.* **70**: 3189–3197.
19. Koyanagi, Y., Miles, S., Mitsuyasu, R. T., Merrill, J. E., Vinters, H. V. and Chen, I. S. Y. 1987. *Science* **236**: 819–822.
20. Kuwata, T., Igarashi, T., Ido, E., Jin, M., Mizuno, A., Chen, J. and Hayami, M. 1995. *J. Gen. Virol.* **76**: 2181–2191.
21. Luciw, P. A., Pratt, L. E., Shaw, K. E., Levy, J. A. and Cheng-Mayer, C. 1995. *Proc. Natl. Acad. Sci. U. S. A.* **92**: 7490–7494.
22. Mori, K., Rosenzweig, M. and Desrosiers, R. C. 2000. *J. Virol.* **74**: 10852–10859.
23. Morner, A., Bjorndal, A., Albert, J., Kewalramani, V. N., Littman, D. R., Inoue, R., Thorstensson, R., Fenyo, E. M. and Bjorling, E. 1999. *J. Virol.* **73**: 2343–2349.
24. O'Brien, W. A., Koyanagi, Y., Namazie, A., Zhao, J. Q., Diagne, A., Idler, K., Zack, J. A. and Chen, I. S. Y. 1990. *Nature (Lond.)* **348**: 69–73.
25. Reimann, K. A., Li, J. T., Veazey, R., Halloran, M., Park, I. W., Karlsson, G. B., Sodroski, J. and Letvin, N. L. 1996. *J. Virol.* **70**: 6922–6928.
26. Shibata, R., Maldarelli, F., Siemon, C., Matano, T., Parta, M., Miller, G., Fredrickson, T. and Martin, M. A. 1997. *J. Infect. Dis.* **176**: 362–373.
27. Smyth, R. J., Yi, Y., Singh, A. and Collman, R. G. 1998. *J. Virol.* **72**: 4478–4484.
28. Ui, M., Kuwata, T., Igarashi, T., Miyazaki, Y., Tamaru, K., Shimada, T., Nakamura, M., Uesaka, H., Yamamoto, H. and Hayami, M. 1999. *J. Med. Primatol.* **28**: 242–248.

Journal of General Virology (2003), 84, 1641–1648 DOI 10.1099/vir.0.18865-0

Mutational analysis of two zinc-finger motifs in the nucleocapsid protein of simian immunodeficiency virus mac239

Wataru Akahata, Eiji Ido and Masanori Hayami

Correspondence
Eiji Ido
eido@virus.kyoto-u.ac.jp

Laboratory of Viral Pathogenesis, Institute for Virus Research, Kyoto University, 53 Shogoin-Kawahara-cho, Kyoto 606-8507, Japan

To clarify the physiological function of two zinc-finger (ZF) motifs in the nucleocapsid (NC) protein of simian immunodeficiency virus (SIV), we constructed three mutant viruses with alterations in either or both motifs using a molecular clone of SIVmac (SIVmac239). An immunoblot analysis of the cell lysates transfected with DNA mutated in either the first (ZF1) or second (ZF2) motif showed that the amount of partially processed Gag products (Pr46) was greater than that produced by the wild-type (WT). The genomic RNA contents in the viral particles released from the transfected cells were measured by quantitative RT-PCR. Values for the ZF1 and ZF2 mutants and the double mutant were 26, 20 and 7 % that of the WT, respectively, indicating that the two ZF motifs of SIVmac239 NC protein function almost equivalently with respect to RNA encapsidation and processing of Gag precursors. Despite the presence of some genomic RNA in the mutant viruses, they lost all viral infectivity. To determine the reason for this, we examined (using PCR) to which step viral DNA synthesis proceeded in the mutant viruses. We did not see any block up to the step of minus-strand DNA synthesis. However, plus-strand DNA synthesis after plus-strand transfer did not occur in any of the mutant viruses. These findings indicated that the mutations in the ZF motifs of SIVmac led to a loss of infectivity due partly to impairment of DNA synthesis, in addition to inefficient encapsidation of genomic RNA.

Received 30 September 2002
Accepted 24 February 2003

INTRODUCTION

Retroviruses possess nucleocapsid (NC) proteins, which bind to genomic RNA in the virion cores (Meric *et al.*, 1984; Stewart *et al.*, 1990) and play various roles during the retrovirus life cycle. Early reports described their importance in interactions with genomic RNA such as genomic encapsidation (Aldovini & Young, 1990; Allain *et al.*, 1994; Darlix *et al.*, 1995; Dorfman *et al.*, 1993; Gorelick *et al.*, 1990, 1993; Meric & Goff, 1989), mediation of RNA dimerization (Prats *et al.*, 1990) and annealing of the primer tRNA to its binding site on the viral RNA (Allain *et al.*, 1994; Barat *et al.*, 1989, 1993; Berkowitz *et al.*, 1993; Prats *et al.*, 1988, 1990, 1991). NC proteins of all retroviruses except spumavirus (Maurer *et al.*, 1988) are known to possess one or two zinc finger (ZF) motifs (Cys-X2-Cys-X4-His-X4-Cys) (Berg, 1986; Covey, 1986). The function of the ZF motifs has been studied in various retroviruses. Site-directed mutagenesis of the ZF motifs in murine leukaemia virus (MuLV) (Gorelick *et al.*, 1988; Meric & Goff, 1989), rous sarcoma virus (Meric *et al.*, 1988) and human immunodeficiency virus type 1 (HIV-1) (Aldovini & Young, 1990; Dorfman *et al.*, 1993; Gorelick *et al.*, 1990) severely reduced encapsidation of genomic RNA and produced non-infectious virus particles, indicating that these motifs are involved in packaging of genomic RNA into budding-out particles at the late stage of virus replication. Moreover, recent reports have delineated the involvement of the ZF motifs in the steps of minus- and plus-strand transfer (Gorelick *et al.*, 1996; Guo *et al.*, 1997), formation of virions and synthesis of the end of the proviral DNA (Tanchou *et al.*, 1998).

One approach to understanding the function of the ZF motifs of retroviruses is to analyse the ZF motifs of other retroviruses. However, the functions of the ZF motifs of other retroviruses are so diverse that it is not easy to generalize. For example, MuLV NC protein has only one motif, whereas HIV-1 NC protein has two. The two ZF motifs in HIV-1 are not functionally equivalent: the first motif (ZF1) is responsible for RNA encapsidation and viral core morphogenesis and the second (ZF2) has a role in Gag polyprotein stability (Dannull *et al.*, 1994; Gorelick *et al.*, 1990, 1993; Mizuno *et al.*, 1996). Furthermore, HIV-1 and HIV-2 differ in the mechanism used for selection of genomic RNA for encapsidation (Garzino-Demo *et al.*, 1995; Kaye & Lever, 1999), although their NC proteins have two consecutive ZF motifs and their amino acid sequences are highly homologous. Simian immunodeficiency virus (SIV) NC protein also has two ZF motifs. Although a few studies have

examined SIV NC protein (Gorelick *et al.*, 1999; Urbaneja *et al.*, 2000; Yovandich *et al.*, 2001), much remains to be learned about the function of its ZF motifs, especially in comparison with those of HIV-1 and HIV-2.

The objective of this study was to analyse the functions of both ZF motifs of SIVmac239. We constructed three NC protein mutants of SIVmac239 with alterations in either or both of the ZF motifs in a manner similar to that used in an analysis of HIV-1 NC protein (Mizuno *et al.*, 1996). We found that the two ZF motifs of SIVmac239 NC functioned almost equivalently in terms of RNA encapsidation, processing of Gag precursors and proviral DNA synthesis. This was in contrast to previous findings for HIV-1 NC proteins where the respective ZF motifs do not function equivalently.

METHODS

Plasmid construction. An infectious molecular clone of SIVmac239 (pMA239) (Kestler *et al.*, 1990; Shibata *et al.*, 1991) was used as a parent proviral DNA. The *Bam*HI–*Pvu*II fragment (nt 2106–2705), which includes a part of the *gag* open reading frame, was subcloned between the sites of *Bam*HI and *Hin*cII in pUC119, and using this plasmid as a template, site-directed mutagenesis of the ZF motifs was performed by PCR as follows. To generate the first ZF motif mutant (designated SIVmac ZF1*), in which the first two cysteine residues in the motif were replaced by serine residues, PCR was performed using the oligonucleotide 5′-TGGGGCTCTGCATTGCCTTGCAGAGTGTC CCTCTTTCCCA**GAATTC**CAAGACTTAATTGGC-3′ (nt 2475–2535) and M13 primer M4 5′-GTTTTCCCAGTCACGAC-3′. This oligonucleotide was designed to create an *Eco*RI site (indicated in bold) in addition to alteration of the amino acids. The underlined letters represent the changed nucleotides. The product amplified by PCR was separated by electrophoresis on an agarose gel and purified using a GENECLEAN II kit (BIO 101). The fragment was then digested with *Bam*HI (nt 2106) and *Ban*II (nt 2533). Another fragment obtained from the plasmid pUC119 harbouring the *Bam*HI–*Pvu*II fragment of SIVmac239 (nt 2106–2705) was also digested with *Ban*II and *Pvu*II. These two fragments, *Bam*HI–*Ban*II (nt 2106–2533) and *Ban*II–*Pvu*II (nt 2533–2705), were subcloned consecutively between the *Bam*HI site and the *Hin*cII site of pUC119. The generated plasmid was then digested with *Bam*HI and *Ppu*MI (nt 2698) and the obtained *Bam*HI–*Ppu*MI fragment was reinserted into the corresponding position in a pUC119 plasmid harbouring the *Bam*HI–*Sse*8387I fragment of SIVmac239 (nt 2105–3402). The generated plasmid was digested with *Bam*HI and *Sse*8387I and the obtained *Bam*HI–*Sse*8387I fragment (nt 2105–3402) was reinserted into the corresponding position in pMA239 to generate the full-sized genome plasmid for SIVmac ZF1*.

To generate the second ZF mutant (designated as SIVmac ZF2*), in which the first two cysteine residues in the second motif were replaced by serine residues, PCR was performed using the oligonucleotide 5′-CAGAGCCCCAAGAAGACAG**GGATCC**TGGAAATCTGGAAAAAT-GGACC-3′ (nt 2526–2572) and M13 primer M4. This oligonucleotide was designed to create a *Bam*HI site (indicated in bold). The underlined letters represent the changed nucleotides. The fragment generated by PCR was digested with *Ban*II (nt 2533) and *Pvu*II (nt 2705). Another fragment obtained from plasmid pUC119 harbouring the *Bam*HI–*Pvu*II fragment of SIVmac239 (nt 2106–2705) was digested with *Bam*HI and *Ban*II. These two fragments, *Bam*HI–*Ban*II (nt 2106–2533) and *Ban*II–*Pvu*II (nt 2533–2705), were subcloned consecutively between the *Bam*HI site and the *Hin*cII site of pUC119. The generated plasmid was then digested with *Bam*HI and *Ppu*MI (nt 2698) and the obtained *Bam*HI–*Ppu*MI fragment was reinserted into the corresponding position in pMA239 in a similar manner to generate the full-sized genome plasmid for SIVmac ZF2*.

To generate the mutant of both ZF motifs (designated as SIVmac ZF1*2*), the *Bam*HI–*Ban*II (nt 2106–2533) and *Ban*II–*Pvu*II (nt 2533–2705) fragments possessing the respective mutations were subcloned consecutively between the *Bam*HI site and the *Hin*cII site of pUC119. The generated plasmid was then digested with *Bam*HI and *Ppu*MI and the obtained *Bam*HI–*Ppu*MI fragment (nt 2106–2698) was reinserted into the corresponding position in pMA239 to generate the full-sized plasmid for SIVmac ZF1*2*.

The sequences of the three generated full-sized genome plasmids were confirmed by sequence analysis in the mutated regions from the *Bam*HI site to the *Pvu*II site (nt 2106–2705) and by digestion with *Eco*RI and *Bam*HI, which can differentiate the respective genomic constructs. The *Eco*RI and *Bam*HI sites were purposely incorporated without any change of amino acid sequence.

Cell culture and transfections. Cos-1 cells were cultured in Dulbecco's modified Eagle's medium (DMEM) containing 10% foetal bovine serum (FBS). The cells were transfected by the DEAE-dextran method (Naidu *et al.*, 1988) with 5 μg of wild-type (WT) or mutant viral plasmid DNAs for a reverse transcriptase (RT) assay to analyse the amount of $p27^{CA}$ using ELISA and for immunoblot analysis of transfected cells. For immunoblot analysis of virus particles and Northern blot analysis of viral RNA, the cells were transfected with a FuGENE 6 Transfection Reagent kit (Roche Diagnostics) with 20 μg of the WT or mutant viral plasmid DNAs following the manufacturer's recommendations.

Reverse transcriptase assay and ELISA. The RT assay was performed as described previously (Willey *et al.*, 1988). The amount of $p27^{CA}$ in the culture supernatant was measured with an ELISA kit (Coulter SIV core antigen assay; Coulter).

Immunoblot analysis. The immunoblot analysis was performed as described previously (Mizuno *et al.*, 1996). For immunoblot analysis of transfected cells, the cells were washed three times 3 days after transfection, suspended in lysis buffer and boiled for 3 min. The samples were fractionated by 5–20% gradient SDS-PAGE (Atto) and transferred to an Immobilon polyvinylidene difluoride membrane (Millipore). Plasma from a SHIV-NM-3rN-infected monkey (Kuwata *et al.*, 1995) was used to provide the first antibody, since high titres of antibodies against SIVmac 239 Gag proteins have been raised in this monkey. For visualization, an ECL system (Amersham) was used with goat anti-human immunoglobulins linked to horseradish peroxidase. To analyse the processing of virus particle-incorporated proteins, the transfected culture supernatant was filtered through a 0·45 μm pore size filter. Each sample was adjusted to contain an equal amount of RT activity in the supernatant. The released viral particles were pelleted by centrifugation at 14 000 r.p.m. for 2 h at 4 °C. The pelleted virions were lysed in lysis buffer and subjected to immunoblot analysis.

Quantitative RT-PCR. For measurement of the genomic RNA in the viral particles and in the cell, we performed quantitative RT-PCR. The transfected culture supernatant was filtered through a 0·45 μm pore size filter and viral RNA was extracted using the QIAamp viral RNA Mini Kit (Qiagen). For the measurement of viral RNA in the cell, the genomic RNA was extracted with Trizol (Gibco BRL). To remove contaminating plasmid DNA, the precipitated RNA was digested with DNase I (Gibco BRL) for 15 min at 37 °C, followed by heat treatment (70 °C, 15 min) to inactivate DNase I. DMEM containing 10 μg pMA239 was also digested with DNase I as a negative control to ensure complete removal of contaminating

plasmid DNA. RT reactions and subsequent PCR conditions were performed with a Taqman RT-PCR kit (Perkin Elmer) according to the manufacture's recommendations. For *gag* region measurement, SIVII-696F 5′-GGAAATTACCCAGTACAACAAATAGG-3′ and SIVII-784R 5′-TCTATCAATTTTACCCAGGACTTTA-3′ were used as primers and the labelling probe SIVII-731 5′-Fam-TGTCCACCTGCCA TTAAGCCCG-Tamra-3′ (Perkin Elmer) was used (Akahata *et al.*, 2000; Suryanarayana *et al.*, 1998). For *nef* region measurement, SIV-9F 5′-AGCTATTTCCATGAGGCGGT-3′ and SIV-84R 5′-ATAAGT CTCCCCACGCGC-3′ were used as primers and the labelling probe SIV-34T 5′-Fam-CCGTCTGGAGATCTGCGACAGAGAC-Tamra-3′ (Perkin Elmer) was used. Each sample was adjusted to contain an equal amount of RT activity in the supernatant before RT-PCR measurement.

RNA blot analysis. Virus particles were pelleted by ultracentrifugation using an SW41 rotor (Beckman Fullerton) at 27 000 r.p.m. for 2 h at 4 °C. Each sample was adjusted to contain an equal amount of RT activity in the supernatant before centrifugation. The viral RNA was extracted with Trizol (Gibco BRL). To remove contaminating plasmid DNA, the precipitated RNA was digested with DNase I (Gibco BRL) for 15 min at 37 °C and then 1 μl 25 mM EDTA was added to inactivate the DNase I. Each sample was denatured, electrophoresed and transferred to a nitrocellulose filter. The *KpnI–KpnI* fragment of pMA239 (nt 1198–4714) was ^{32}P-labelled by the random probing method using a commercial labelling kit (Ambion) and used as a hybridization probe.

Viral DNA detection. M8166 cells (5×10^5 cells), a human CD4-positive lymphoid cell line, were infected with the virus stock for 4, 8 and 48 h at 37 °C in a six-well plate. Each virus stock was collected from the supernatant of the Cos-1 cells transfected with either the WT or the mutant full-sized genome plasmid and each stock was filtered through a 0·45 μm pore size filter and adjusted to contain an equal amount of viral RNA in the supernatant. For adjustment of the amount of viral RNA in the each stock, quantitative RT-PCR in the *gag* region was performed before infection. After 4, 8 and 48 h infection, M8166 cells were washed three times with PBS, mixed with 2 U DNase I (Gibco BRL) and incubated for 15 min at 37 °C to remove contaminating plasmid DNA. DNA was then extracted using the QIAamp DNA Mini kit (Qiagen). PCR was carried out using extracted DNA obtained from 5×10^4 cells using the following five primer pairs: (i) R/U5 PCR of viral DNA [synthesis of minus strong-stop DNA (−ssDNA)] by LTR Rf 5′-TTCTCTCCAGC ACTAGCAGGTAGAGCCTGGGTGTTCCCTG-3′ (nt 816–855) and LTR U5r 5′-CAGGCGCCAATCTGCTAGGGATTTTCCTGCTTC-3′ (nt 1054–1086) primers; (ii) U3/U5 PCR of viral DNA (elongation of minus-strand DNA after the minus-strand transfer) by LTR 2F 5′-GGAGCCGGTCGGGAACGCCCACTTTCTTGATGTAT-3′ (nt 712–746) and LTR U5r primers; (iii) CA/MA minus-strand DNA by HP1 5′-TTAGGCTACGACCCGGCGGAAAGA-3′ (nt 1364–1387) and MG1655R 5′-TGCATAGCCGCTTGATGGTCTCCCACAC-3′ (nt 1883–1910) primers (end of the minus-strand DNA synthesis); (iv) U3/CA of viral DNA by LTR 2F and MG1655R primers (elongation of plus-strand DNA after plus-strand transfer); and (v) 2-LTR PCR of viral DNA by LTR 2F and MLTR 5R 5′-CCCGCTCGAG TGGTATGATGCCTTCTTCCTTTTCTAAGTA-3′ (nt 304–343) primers. The primer pairs in (ii), (iv) and (v) have been used previously (Xiao *et al.*, 2000). After denaturation of the template DNA at 96 °C for 5 min, the DNA was amplified for 40 cycles under the following conditions: denaturation at 96 °C for 60 s, annealing at 60 °C for 60 s and extension at 72 °C for 60 s. For the primer pairs in (iv), extension at 72 °C was prolonged for 120 s. A final extension at 72 °C for 5 min was added to the last cycle.

RESULTS

Plasmid construction

To investigate the individual roles of the two ZF motifs (Cys-X2-Cys-X4-His-X4-Cys) in virus replication, we constructed a series of mutant proviral DNAs with alterations to amino acid residues in the respective motifs. To minimize the effects that these changes had on the conformation of the NC protein, we replaced the first two cysteine residues in the respective fingers with serine residues because of the similarity between the two side-chains. The mutants for ZF1 and ZF2 and the double ZF mutant were named SIVmac ZF1*, SIVmac ZF2* and SIVmac ZF1*2*, respectively.

Viral protein production

To examine viral protein production by the mutant proviral DNAs, Cos-1 cells were transfected with each plasmid, and the RT activity and amount of $p27^{CA}$ in the supernatants were measured. Table 1 summarizes the RT activity and amounts of $p27^{CA}$ 3 days after transfection. In comparison with the WT, we observed approximately the same or slightly lower levels of RT activity and amounts of $p27^{CA}$ in SIVmac ZF1* and SIVmac ZF2*. However, the level of RT activity and amount of $p27^{CA}$ were extremely low in SIVmac ZF1*2* (approximately 20 % that of the WT).

Viral protein processing in transfected cells and in particles

Processing of the viral proteins by the mutant proviral DNAs in Cos-1 cells was examined by Western immunoblot

Table 1. Production of SIVmac239 viral proteins in supernatants of transfected cells

Days after transfection	$10^{-2} \times$ RT activity (c.p.m. ml^{-1})†					p27 (ng ml^{-1})‡			
	WT	ZF1*	ZF2*	ZF1*2*	Mock	WT	ZF1*	ZF2*	ZF1*2*
1	80	62	77	48	27	116	55	84	69
2	214	161	202	59	37	399	334	434	88
3	283	183	254	46	27	464	421	460	83

†The values given are the mean of three experiments.

‡The amount of $p27^{CA}$ was measured using an SIV $p27^{CA}$ antigen capture assay kit. The values given are the mean of two experiments.

analysis. Cos-1 cells were transfected with equal amounts of the WT and mutant DNAs. Three days after transfection, the cells were lysed. As a source of first antibody, we used plasma from an SHIV-NM-3rN-infected monkey. Antibodies in this plasma can detect the SIVmac239 Gag precursor protein, Pr56, and a partially processed precursor, Pr46 ($p17^{MA}$ and $p27^{CA}$), as well as $p27^{CA}$, since SHIV-NM-3rN is a chimeric virus and its *gag* region is derived from SIVmac239. As shown in Fig. 1, the amounts of Pr46 in the cell lysates transfected with both SIVmac ZF1* and SIVmac ZF2* were greater than that for the WT. The cell lysates transfected with SIVmac ZF1*2* contained greatly reduced levels of Pr46 and $p27^{CA}$.

To investigate the effects of the mutations on particle maturation after the budding step, virus particles produced by the mutant DNAs were pelleted and subjected to immunoblot analysis. The samples were adjusted so that they had equal amounts of RT activity prior to the immunoblot analysis. Each of the mutant particles was found to contain amounts of $p27^{CA}$, $p17^{MA}$ and unprocessed Gag precursor proteins approximately equal to the WT (Fig. 2).

Taken together, these results indicate that the viruses were influenced by the ZF mutations shown by the delayed processing of Gag precursors in the transfected cells before budding out. However, viral particles in all the mutants appeared to incorporate viral proteins that were processed normally during the budding step.

Analysis of genomic RNA

Based on an analysis of the *gag* region of genomic RNA by quantitative RT-PCR, the RNA contents in the viral particles produced by the SIVmac ZF1*, ZF2* and ZF1*2* DNAs were 26, 20 and 7 % that of the WT, respectively (Fig. 3). A similar analysis based on the *nef* region of genomic RNA by quantitative RT-PCR gave similar results (data not shown). We also measured the genomic RNA level in the cells 3 days post-transfection and found no significant difference in the RNA levels among the three mutants and the WT (data not shown). A Northern blot analysis was attempted to detect unspliced viral RNA. Unspliced genomic RNA was seen for the WT. However, unspliced genomic RNA was not clearly

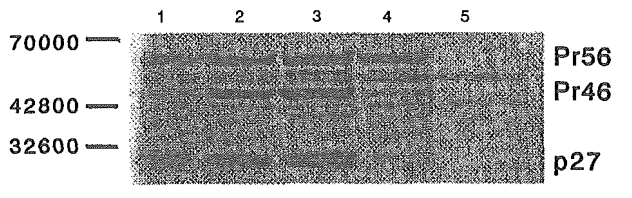

Fig. 1. Immunoblot analysis of processing of Gag proteins by WT and mutant DNAs in transfected Cos-1 cells. At 72 h post-transfection, Cos-1 cells were suspended in lysis buffer. The samples were fractionated by 5–20 % gradient SDS-PAGE. Lane 1, WT; lane 2, SIVmac ZF1*; lane 3, SIVmac ZF2*; lane 4, SIVmac ZF1*2*; lane 5, mock-infected cells. Molecular mass markers (Da) are shown on the left.

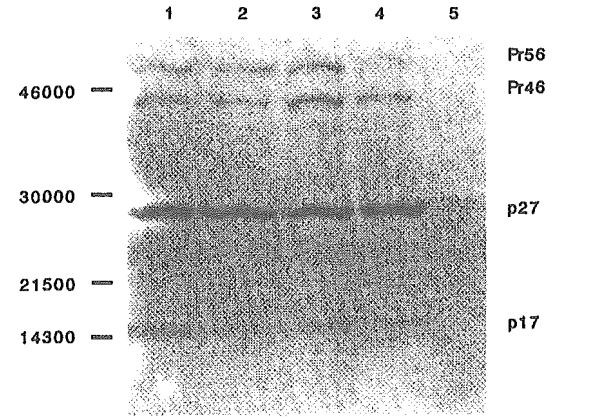

Fig. 2. Immunoblot analysis of virus particles produced by WT and mutant DNAs. Culture supernatants were collected 24–72 h post-transfection, filtered and adjusted to contain equal amounts of RT activity. The released viral particles were pelleted by centrifugation. The pelleted virions were lysed and fractionated by 5–20 % gradient SDS-PAGE. Lane 1, WT; lane 2, SIVmac ZF1*; lane 3, SIVmac ZF2*; lane 4, SIVmac ZF1*2*; lane 5, mock-infected cells. Molecular mass markers (Da) are shown on the left.

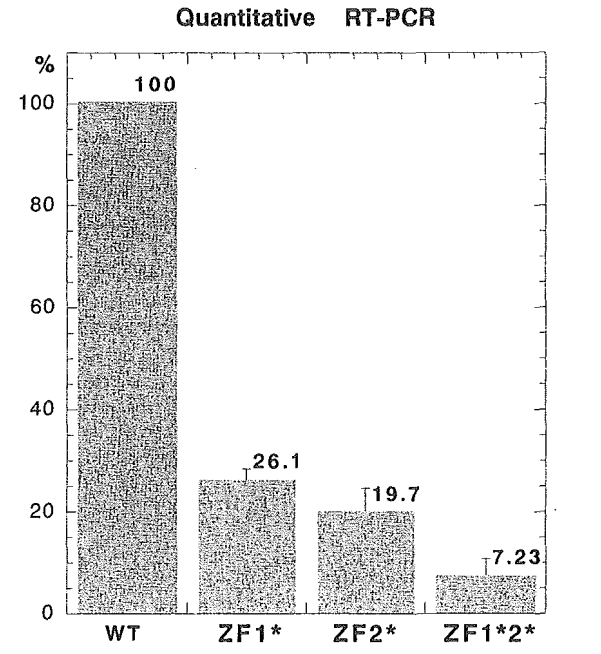

Fig. 3. Viral RNA content in the WT and mutant viral particles measured by quantitative RT-PCR. The average amount of viral RNA in the WT was arbitrarily set at 100 %. Each average value and standard deviation was determined from four independent experiments.